Certified Reduced Basis Methods for Parametrized Parabolic Partial Differential Equations with Non-Affine Source Terms

Dirk Klindworth[a], Martin A. Grepl[b,*], Georg Vossen[a]

[a] *RWTH Aachen University, Nonlinear Dynamics of Laser Processing, Steinbachstraße 15, 52074 Aachen, Germany*
[b] *RWTH Aachen University, Numerical Mathematics, Templergraben 55, 52056 Aachen, Germany*

Abstract

We present rigorous *a posteriori* output error bounds for reduced basis approximations of parametrized parabolic partial differential equations with non-affine source terms. The method employs the empirical interpolation method in order to construct affine coefficient-function approximations of the non-affine parametrized functions. Our *a posteriori* error bounds take both error contributions explicitly into account — the error introduced by the reduced basis approximation *and* the error induced by the coefficient function interpolation. To this end, we employ recently developed rigorous error bounds for the empirical interpolation method and develop error estimation and primal-dual formulations to provide rigorous bounds for the error in specific outputs of interest. We present an efficient offline-online computational procedure for the calculation of the reduced basis approximation and associated error bound. The method is thus ideally suited for many-query or real-time contexts. As a specific motivational example we consider a three-dimensional mathematical model of a welding process. Our numerical results show that we obtain efficient and reliable mathematical models which may be gainfully employed in manufacturing and product development.

Keywords:
reduced basis methods, parabolic PDEs, non-affine parameter dependence, *a posteriori* error estimation, empirical interpolation method, welding process

*Corresponding author. Tel.: +49 241 8096470, Fax: +49 241 80696470
Email address: grepl@igpm.rwth-aachen.de (Martin A. Grepl)

1. Introduction

The role of numerical simulation in engineering and science has become increasingly important. System or component behavior is often modeled using a set of parametrized partial differential equations (PDEs) and associated boundary and initial conditions, where the parameters, or inputs, μ — such as material properties and geometry — serve to identify a particular configuration. Since the analytical solution to these problems is generally unavailable, a discretization procedure such as the finite element method (FEM) is used in practice. In a design, optimization, and control context one often requires repeated, reliable, and real-time prediction of the system or component outputs, s^{e}, such as heat fluxes or flow rates[1]. These outputs are typically functionals of field variables, y^{e} — such as temperatures or velocities — associated with the parametrized PDE. The relevant system behavior is thus described by an implicit input-output relationship, $s^{\mathrm{e}}(\mu)$, evaluation of which demands solution of the underlying parametrized PDE.

More specifically, the motivation of this work is to develop an efficient mathematical model for the heat flow in a welding process [1, 2, 3, 4, 5]. An accurate knowledge of the temperature distribution within the workpiece is crucial in determining the quality of the weld: two such quality measures are the weld pool depth — indicating the strength of the joint — and the shape distortion of the workpiece.

A complete model of the welding process which couples and accounts for all of the physical processes involved does not yet exist. In actual practice, the heat flux input is therefore modeled as a parametrized volume heat source [2, 6, 7]. The non-dimensionalized temperature distribution, $y^{\mathrm{e}}(x,t;\mu)$, within the workpiece is governed by the (appropriately) non-dimensionalized unsteady convection-diffusion equation

$$\frac{\partial}{\partial t}y^{\mathrm{e}}(x,t;\mu) + \mathrm{v}\cdot\nabla y^{\mathrm{e}}(x,t;\mu) - \kappa\nabla^2 y^{\mathrm{e}}(x,t;\mu) = q(x;\mu)\,u(t), \quad x\in\Omega,\ t\in I, \tag{1}$$

with initial condition (say) $y^{\mathrm{e}}(x,t=0;\mu)=0$. Here, $\Omega\subset\mathbb{R}^3$ is the three-dimensional spatial domain, a point in which shall be denoted by $x=(x_1,x_2,x_3)$, the time interval of interest is $I=]0,t_{\mathrm{f}}]$ with final time $t_{\mathrm{f}}>0$, v corresponds to the velocity of the torch[2], κ is the thermal

[1] Here, superscript "e" shall refer to "exact." We shall later introduce a "truth approximation" which will bear no superscript.

[2] We consider a coordinate system moving with the same velocity as the torch. In this coordinate system, the torch is stationary and the velocity enters as a convective term in the governing equation; see Section 3.1.3.

diffusivity, and $u(t)$ is the source strength. In this paper, we consider the so called *hemispherical volume heat source* given by

$$q(x;\mu) := e^{-x_1^2/\sigma_1^2}\ e^{-x_2^2/\sigma_2^2}\ e^{-x_3^2/\sigma_3^2}, \qquad x \in \Omega. \tag{2}$$

The standard deviations $\sigma_i,\ i = 1, 2, 3$, and the thermal diffusivity κ shall serve as our parameter, i.e., our parameter of interest is $\mu = (\sigma_1, \sigma_2, \sigma_3, \kappa)$. The source type (2) is a special case of the *double ellipsoid source* which was first introduced by Goldak et al. [6] to model the heating effect of a welding torch. We note, however, that the methods developed in this paper are not restricted to the particular welding process considered here, i.e., Gaussian source terms play an important role in many applications in science and engineering — another prominent example is the simulation of airborne contaminants [8, 9, 10]. Furthermore, our approach of course also directly applies to other types of non-affine functions besides Gaussians.

The main task in the analysis and modeling of the welding process is to find parameters $(\sigma_1, \sigma_2, \sigma_3)$ such that the simulated temperature at one or several measurement points on the surface of the workpiece predicted by (1) and (2) matches the experimental measurements [11]. Given the parameter estimates, we may subsequently aim to control the welding process to achieve a desired weld pool depth [12, 13, 3]. The parameter estimation problem needs to be solved in real-time, requiring a rapid and reliable evaluation of the PDE (1). Our goal here is thus to develop numerical methods to efficiently and reliably evaluate the forward problem, i.e, the PDE-induced input output relationship (1), in the limit of many queries or in real-time.

To achieve this goal we pursue the reduced basis method. The reduced basis method is a model-order reduction technique which provides efficient yet reliable approximations to solutions of parametrized partial differential equations in the many-query or real-time context; see [14] for a recent review of contributions to the methodology. In this paper we focus on parabolic problems with a *non-affine* parameter dependence in the source term — a typical example is given by the Gaussian function (2). To this end we employ the empirical interpolation method (EIM) [15] which serves to construct affine approximations of non-affine parametrized functions. The method is frequently applied in reduced basis approximations of parametrized PDEs with non-affine parameter dependence [15, 16, 17, 18, 19]; the affine approximation of the coefficient function is crucial for computational efficiency.

A posteriori error estimators for non-affine elliptic and parabolic problems have been proposed

in [17, 19] and [20], respectively. However, these estimators do not provide a provable rigorous upper bound for the true error due to the contribution of the interpolation error. Only recently, Eftang et al. [21] introduced a rigorous error analysis for the EIM. Furthermore, reduced basis output approximations and associated output bounds may suffer from a slow convergence, thus requiring a large dimension of the reduced order model to achieve a desired accuracy. Primal-dual formulations were proposed in [22] to circumvent this problem and improve the accuracy of the output prediction. These ideas have been successfully applied also in the FEM context, e.g. in [23, 24], and in the reduced basis context, e.g. in [25, 26, 27]. However, these previous reduced basis works only considered *affine* problems. The contributions here are thus (i) rigorous *a posteriori* error bounds for reduced basis approximations of non-affine parabolic problems, and (ii) the development of primal-dual formulations for non-affine problems to ensure rapid convergence of the reduced basis output approximation and output error bound.

This paper is organized as follows: in Section 2 we present a short review of the EIM and corresponding rigorous error analysis. The abstract problem formulation and reduced basis approximation for linear coercive parabolic problems with non-affine source terms are introduced in Section 3. In Section 4 we develop our *a posteriori* error estimation procedures and in Section 5 we briefly discuss the sampling technique to generate the reduced basis space. Numerical results for the welding process are presented in Section 6. Finally, we offer concluding remarks in Section 7.

2. Empirical Interpolation Method

In this section we briefly review the EIM and associated *a posteriori* error estimation procedures [15, 16, 21].

2.1. Coefficient Function Approximation

We assume we are given a function $g\colon \Omega \times \mathcal{D} \to \mathbb{R}$ with $g(\cdot;\mu) \in L^\infty(\Omega)$ for all $\mu \in \mathcal{D}$, where $\mathcal{D} \subset \mathbb{R}^P$ is the set of admissible parameters, $\Omega \subset \mathbb{R}^d$, $d = 1, 2, 3$, is a bounded domain, and $L^\infty(\Omega) := \{v \,|\, \operatorname{ess\,sup}_{v\in\Omega} |v(x)| < \infty\}$. We introduce a finite but suitably large parameter train sample $\Xi^{\text{EIM}}_{\text{train}} \subset \mathcal{D}$ which shall serve as our surrogate for $\mathcal{D}$, and a triangulation $\mathcal{T}_{\mathcal{N}}(\Omega)$ of Ω with $\mathcal{N}$ vertices over which we shall in practice realize $g(\cdot;\mu)$ as a piecewise linear function.

The construction of the EIM approximation space W_M^g and set of interpolation points $T_M^g = \{\hat{x}^1, \ldots, \hat{x}^M\}$ is based on a greedy algorithm [28]: we first choose $\mu^1 := \arg\max_{\mu \in \Xi_{\text{train}}^{\text{EIM}}} \|g(\cdot;\mu)\|_{L^\infty(\Omega)}$, set $\hat{x}^1 := \arg \operatorname{ess\,sup}_{x\in\Omega} \left|g(x;\mu^1)\right|$, and obtain the first (normalized) EIM basis function $\hat{g}^1(x) := g(x;\mu^1)/g(\hat{x}^1;\mu^1)$. We define $W_1^g := \operatorname{span}\left\{\hat{g}^1(\cdot)\right\}$ and introduce the nodal value matrix $G^1 \in \mathbb{R}^{1\times 1}$ with the single element $G^1_{1,1} := \hat{g}^1(\hat{x}^1) = 1$.

Then, for $1 \le M \le M_{\max} - 1$, we compute the approximation $g_M(\cdot;\mu)$ to $g(\cdot;\mu)$ from

$$g_M(x;\mu) := \sum_{m=1}^{M} \omega_m(\mu)\hat{g}^m(x), \tag{3}$$

where the coefficient vector $\underline{\omega}(\mu) = [\omega_1(\mu), \ldots, \omega_M(\mu)]^{\mathrm{T}} \in \mathbb{R}^M$ is given by the solution of the linear system

$$G^M \underline{\omega}(\mu) = \left[g(\hat{x}^1;\mu), \ldots, g(\hat{x}^M;\mu)\right]^{\mathrm{T}}. \tag{4}$$

We choose the next parameter

$$\mu_{M+1} := \arg \max_{\mu\in\Xi_{\text{train}}^{\text{EIM}}} \|g(\cdot;\mu) - g_M(\cdot;\mu)\|_{L^\infty(\Omega)} \tag{5}$$

and define the residual $r_M^g(x) := g(x;\mu_{M+1}) - g_M(x;\mu_{M+1})$. The next interpolation point is then set to $\hat{x}^{M+1} := \arg\max_{x\in\Omega} \left|r_M^g(x)\right|$, and the next EIM basis function is given by $\hat{g}^{M+1}(x) := r_M^g(x)/r_M^g(\hat{x}^{M+1})$. We define $W_{M+1}^g := \operatorname{span}\{\hat{g}^m(\cdot) \,|\, 1 \le m \le M+1\}$, and update our nodal value matrix $G^{M+1} \in \mathbb{R}^{(M+1)\times(M+1)}$ with components $G^{M+1}_{m,n} := \hat{g}^n(\hat{x}^m)$, $1 \le m, n \le M+1$. This procedure is either terminated if the maximum dimension of the EIM space $M_{\max}$ is reached or if the maximum of $\|g(\cdot;\mu) - g_M(\cdot;\mu)\|_{L^\infty(\Omega)}$ over all $\mu \in \Xi_{\text{train}}^{\text{EIM}}$ is smaller than some desired tolerance $\varepsilon_{\text{tol}} > 0$. We note that the determination of the coefficients $\underline{\omega}(\mu)$ requires only $\mathcal{O}(M^2)$ computational cost since G^M is lower triangular with unity diagonal and that $\{\hat{g}^m\}_{m=1}^M$ is a basis for W_M^g [15, 16].

Finally, we define a "Lebesgue constant" [29] $\Lambda_M := \sup_{x\in\Omega} \sum_{m=1}^M |V_m^M(x)|$, where $V_m^M(x) \in W_M^g$ are the characteristic functions of W_M^g satisfying $V_m^M(x_n) \equiv \delta_{mn}$, $1 \le m, n \le M$; here, δ_{mn} is the Kronecker delta symbol. We recall that *(i)* the set of all characteristic functions $\{V_m^M\}_{m=1}^M$ is a basis for W_M^g, and *(ii)* the Lebesgue constant Λ_M satisfies $\Lambda_M \le 2^M - 1$, see [15, 16]. In applications, the actual asymptotic behavior of Λ_M is much better, as we shall observe subsequently.

2.2. A Posteriori Error Estimation

Given an approximation $g_M(x;\mu)$ to $g(x;\mu)$, we first define the interpolation error as

$$\varepsilon_M^g(\mu) := \|g(\cdot;\mu) - g_M(\cdot;\mu)\|_{L^\infty(\Omega)}\,. \tag{6}$$

We recall that, if $g(\cdot;\mu) \in W_{M+1}^g$, the interpolation error satisfies $\varepsilon_M^g(\mu) = \hat{\delta}_M^g(\mu)$, where the error estimator, $\hat{\delta}_M^g(\mu)$, is defined as $\hat{\delta}_M^g(\mu) := |g(x_{M+1};\mu) - g_M(x_{M+1};\mu)|$, see [15, 16]. Since $\hat{\delta}_M^g(\mu)$ is very inexpensive to evaluate, it is used as an estimator for the function interpolation error in combination with the reduced basis method in the literature so far. However, in general $g(\cdot;\mu) \notin W_{M+1}^g$ and $\hat{\delta}_M^g(\mu)$ is only a lower bound for the true error $\varepsilon_M^g(\mu)$. Due to the condition on $g(\cdot;\mu)$ we refer to this bound as the "next-point" bound.

In a recent note, Eftang et al. [21] proposed a new rigorous *a posteriori* error bound which does not rely on the assumption $g(\cdot;\mu) \in W_{M+1}^g$. We shall assume that g is parametrically smooth; for simplicity here, we suppose $g \in C^\infty(\mathcal{D}, L^\infty(\Omega))$. We first introduce a P-dimensional multi-index $\beta := [\beta_1, \ldots, \beta_P]$ with non-negative integers $\beta_1, \ldots, \beta_P$. We define the length $|\beta| := \sum_{i=1}^P \beta_i$ and refer to $\mathcal{B}_l^P$ as the set of all multi-indices β of dimension P and length $|\beta| = l$. The number of elements of $\mathcal{B}_l^P$ is then given by $\left|\mathcal{B}_l^P\right| = \binom{P+l-1}{l}$. We then define the parametric derivatives

$$g^{(\beta)}(x;\mu) := \frac{\partial^{|\beta|} g(x;\mu)}{\partial\mu_1^{\beta_1}\ldots\partial\mu_P^{\beta_P}}. \tag{7}$$

Note that we use the same interpolation space W_M^g for both the function g and its parametric derivatives.

We further assume that for all non-negative integers p there exists a constant $\sigma_p < \infty$ such that $\max_{\mu\in\mathcal{D}} \max_{\beta\in\mathcal{B}_p^P} \left\|g^{(\beta)}(\cdot;\mu)\right\|_{L^\infty(\Omega)} \le \sigma_p$. We also introduce a finite set of points $\Phi \subset \mathcal{D}$ with $|\Phi|$ elements and define $\rho_\Phi := \max_{\mu\in\mathcal{D}} \min_{\phi\in\Phi} \|\mu - \phi\|_2$; here $\|\cdot\|_2$ is the usual Euclidean norm. For given positive integer p, the interpolation error then satisfies [21]

$$\varepsilon_M^g(\mu) \le \delta_{M,p,\Phi}^g, \qquad \forall\mu \in \mathcal{D}, \tag{8}$$

where the rigorous error bound is given by

$$\delta_{M,p,\Phi}^g := (1+\Lambda_M)\,\frac{\sigma_p}{p!}\rho_\Phi^p P^{p/2} + \sup_{\phi\in\Phi}\left(\sum_{j=0}^{p-1}\frac{\rho_\Phi^j}{j!}P^{j/2}\max_{\beta\in\mathcal{B}_j^P}\left\|g^{(\beta)}(\cdot;\phi) - g_M^{(\beta)}(\cdot;\phi)\right\|_{L^\infty(\Omega)}\right). \tag{9}$$

In practice, higher values of p and larger cardinalities $|\Phi|$ require larger computational effort but result in sharper bounds. However, note that the bound is parameter-independent and can thus be computed *once* offline.

2.3. Numerical Results

In this section we apply the EIM to the *hemispherical volume heat source* defined in (2), given by

$$q(x;\mu) = e^{-x_1^2/\sigma_1^2}\, e^{-x_2^2/\sigma_2^2}\, e^{-x_3^2/\sigma_3^2}, \qquad x \in \Omega, \tag{10}$$

for $x = (x_1, x_2, x_3) \in \Omega := [-30, 10] \times [0, 10] \times [-10, 0]$ and $\mu_q = (\sigma_1, \sigma_2, \sigma_3) \in \mathcal{D}_q := [1.08, 1.32]^3$. Note that the subscript "q" is used to denote the subset of the parameter and parameter domain related to the source term $q(x;\mu)$. The admissible parameter set $\mathcal{D}_q$ is obtained by taking $\bar{\mu}_q = (1.2, 1.2, 1.2)$ from the double ellipsoid source of the penetration welding example in [6] and assuming a 10% uncertainty in each parameter. We perform our computations on a triangulation $\mathcal{T}_\mathcal{N}(\Omega)$ with $\mathcal{N} = 23891$ vertices and 133805 tetrahedra (also see Figure 2 for a sketch of the computational domain).

Next, we choose a random parameter train sample $\Xi_{\text{train}}^{\text{EIM}} \subset \mathcal{D}_q$ with 1000 elements for the greedy algorithm to construct the coefficient-function approximation. For the computation of the rigorous error bound we introduce two deterministic parameter samples $\Phi_1 \subset \mathcal{D}_q$ and $\Phi_2 \subset \mathcal{D}_q$ with $|\Phi_1| = 125$ and $|\Phi_2| = 1000$ elements. We shall consider $p = 1, 2, \ldots, 5$ and test the rigorous error bound with a random parameter test sample $\Xi_{\text{test}}^{\text{EIM}} \subset \mathcal{D}_q$ with 100 elements.

In Figure 1 (a) and (b), we plot the maximum interpolation error $\varepsilon_M^{q,\max} = \max_{\mu_q \in \Xi_{\text{test}}^{\text{EIM}}} \varepsilon_M^q(\mu_q)$ and interpolation error bound $\delta_{M,p,\Phi}^q$ as function of M for $p = 1, 2, \ldots, 5$ and $\Phi = \Phi_1$ and $\Phi = \Phi_2$, respectively. We observe that the error bounds initially decrease, but then reach a plateau in M depending on the particular value of p. The plateau itself is due to the fact that the first term in (9) eventually dominates and compromises the sharpness of the bounds. The slight increase of each plateau is related to the growth of the Lebesgue constant Λ_M with M. We note that with increasing p and increasing $|\Phi|$ the bound is sharper for a larger range of M, thus resulting in smaller effectivities.

In Table 1, we first present the Lebesgue constant Λ_M, the condition number $\kappa(G^M)$ of the nodal value matrix G^M, and the maximum interpolation error $\varepsilon_M^{q,\max}$ as a function of M. We observe that the Lebesgue constant grows very slowly, and that the nodal value matrix G^M is quite well-conditioned. Note that the modest growth of the Lebesgue constant is crucial to obtain a sharp error bound [30]. The maximum interpolation error $\varepsilon_M^{q,\max}$ decreases very fast with M.

We next compare the rigorous error bound and the non-rigorous "next-point" error bound. To

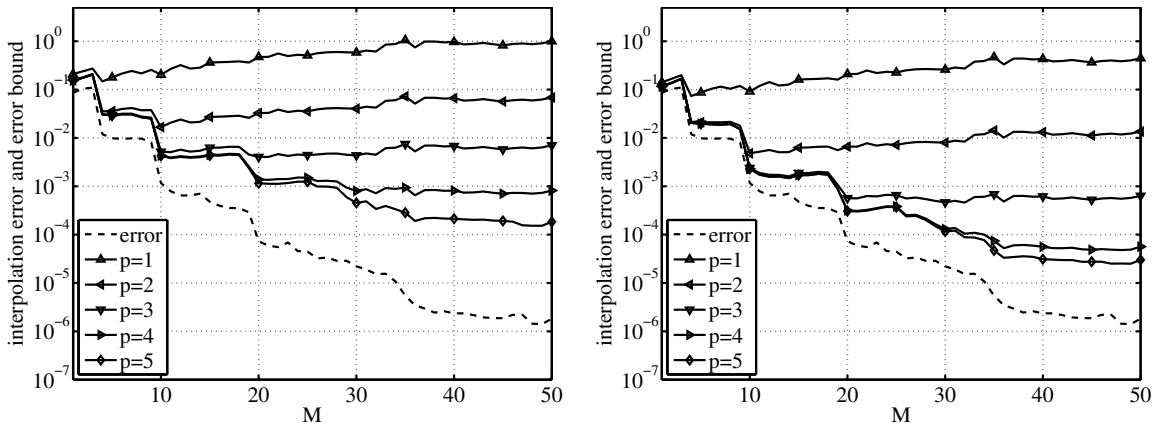

(a) $\Phi = \Phi_1$ with $|\Phi_1| = 125$ (b) $\Phi = \Phi_2$ with $|\Phi_2| = 1000$

Figure 1: Numerical results for the empirical interpolation of $q(x;\mu)$: maximum interpolation error $\varepsilon_M^{q,\max}$ (dashed line) and interpolation error bound $\delta_{M,p,\Phi}^q$ (solid lines) for $p = 1, \ldots, 5$ as a function of M.

this end, we also present in Table 1 the rigorous error bound $\delta_{M,p,\Phi}^q$ and the effectivity $\eta_{M,p,\Phi}^q = \delta_{M,p,\Phi}^q / \varepsilon_M^{q,\max}$ for $p = 5$ and $\Phi = \Phi_2$, as well as the maximum non-rigorous error bound $\hat{\delta}_M^{q,\max} = \max_{\mu_q \in \Xi_{\text{test}}^{\text{EIM}}} \hat{\delta}_M^q(\mu_q)$ and the average effectivity $\hat{\eta}_M^{q,\text{ave}} = (1/|\Xi_{\text{test}}^{\text{EIM}}|) \sum_{\mu_q \in \Xi_{\text{test}}^{\text{EIM}}} \hat{\delta}_M^q(\mu_q)/\varepsilon_M^q(\mu_q)$. We observe that both the rigorous bound $\delta_{M,p,\Phi}^q$ and the non-rigorous bound $\hat{\delta}_M^{q,\max}$ decrease very fast. However, $\delta_{M,p,\Phi}^q$ is a true upper bound for the interpolation error: the effectivity is always larger than one and — as expected — grows slowly with M (note that $\delta_{M,5,\Phi_2}^q$ reaches the plateau for $M = 36$). The non-rigorous error bound, on the other hand, clearly underestimates the interpolation error: the average effectivities are less than one for all values of M. We recall that the offline stage for the rigorous bound is much more expensive than for the "next-point" bound [21]. In the online stage, however, the rigorous bound requires no computation at all and the "next-point" bound requires only one additional evaluation of the non-affine function at a single point in Ω. As long as we can afford the increased offline cost, the rigorous bound is thus clearly preferable.

3. Reduced Basis Method

In this section we incorporate the empirical interpolation method described in the last section into our reduced basis approximation to develop an efficient offline-online computational procedure for linear parabolic problems with non-affine source terms.

M	Λ_M	$\kappa(G^M)$	$\varepsilon_M^{q,\max}$	$\delta^q_{M,5,\Phi_2}$	$\eta^q_{M,5,\Phi_2}$	$\hat{\delta}_M^{q,\max}$	$\hat{\eta}_M^{q,\text{ave}}$
10	2.29	4.96	1.17E-03	2.31E-03	1.98	1.13E-03	0.48
20	6.71	7.57	7.30E-05	3.08E-04	4.22	7.30E-05	0.53
30	8.54	13.86	2.20E-05	1.16E-04	5.26	2.20E-05	0.57
40	14.78	22.78	2.36E-06	3.12E-05	13.20	1.97E-06	0.51
50	15.31	25.32	1.83E-06	3.01E-05	16.49	1.22E-06	0.63

Table 1: Numerical results for the empirical interpolation of $q(x;\mu)$: Lebesgue constant Λ_M, condition number $\kappa(G^M)$, maximum interpolation error $\varepsilon_M^{q,\max}$, rigorous error bound $\delta^q_{M,p,\Phi}$ and associated effectivity $\eta^q_{M,p,\Phi}$ for $p=5$ and $\Phi=\Phi_2$, maximum non-rigorous error bound $\hat{\delta}_M^{g,\max}$ and associated average effectivity $\hat{\eta}_M^{g,\text{ave}}$ as a function of M.

3.1. Problem Formulation

3.1.1. Abstract Statement

We recall that $\Omega \subset \mathbb{R}^d$, $d = 1, 2, 3$, denotes the spatial domain, a particular point in which is denoted by $x = (x_1, \ldots, x_d) \in \Omega$. We also specify the function space $X^{\text{e}} \equiv H^1_0(\Omega)$ — or, more generally $H^1_0(\Omega) \subset X^{\text{e}} \subset H^1(\Omega)$ — where $H^1(\Omega) := \{v \mid v \in L^2(\Omega), \nabla v \in (L^2(\Omega))^d\}$, $H^1_0(\Omega) := \{v \mid v \in H^1(\Omega), v|_{\partial\Omega} = 0\}$, and $L^2(\Omega)$ is the space of square integrable functions over Ω [31].

For simplicity, we will directly consider a time-discrete framework associated to the time interval $I :=]0, t_f]$ ($\bar{I} := [0, t_f]$). We divide $\bar{I}$ into K subintervals of equal length $\Delta t = t_f/K$ and define $t^k := k\Delta t$, $0 \le k \le K = t_f/\Delta t$. We shall apply the finite differences θ-method [29] with $0.5 \le \theta \le 1$ for the time integration and define $v^{k+\theta} \equiv (1-\theta)v^k + \theta v^{k+1}$ for any time-discrete variable v^k, $0 \le k \le K$. Note that $\theta = 1$ corresponds to the Euler-backward and $\theta = 0.5$ to the Crank-Nicolson scheme.

Our exact problem of interest is then: given a parameter $\mu \in \mathcal{D} \subset \mathbb{R}^P$, we evaluate the output

$$s^{\text{e}}(t^k;\mu) = l(y^{\text{e}}(\cdot, t^k;\mu)), \qquad k = 1, \ldots, K, \tag{11}$$

where $y^{\text{e},k}(\mu) \equiv y^{\text{e}}(\cdot, t^k;\mu) \in X^{\text{e}}$ satisfies the weak form of the parametrized linear parabolic PDE

$$m(y^{\text{e},k+1}(\mu) - y^{\text{e},k}(\mu), v) + \Delta t\, a(y^{\text{e},k+\theta}(\mu), v;\mu) = \Delta t\, f(v; g(\cdot;\mu))u^{k+\theta} \tag{12}$$

for all $v \in X^{\text{e}}$ and $k = 0, 1, \ldots, K-1$, with initial condition (say) $y^{\text{e}}(\cdot, 0;\mu) \equiv 0$ for all $\mu \in \mathcal{D}$. Here, $a(\cdot,\cdot;\mu)$ is an X^{e}-continuous bilinear form, $m(\cdot,\cdot) = (\cdot,\cdot)_{L^2(\Omega)}$ is a symmetric $L^2(\Omega)$-continuous

bilinear form, $l(\cdot)$ and $f(\cdot; g(\cdot;\mu))$ are $L^2(\Omega)$-continuous linear forms, $u\colon]0, t_{\rm f}] \to \mathbb{R}$ is the control function, and $g(\cdot;\mu) \in L^\infty(\Omega)$ is a prescribed function which is non-affine with respect to the parameter μ.

We next introduce the X-inner product

$$(v, w)_X = \frac{1}{2}\left(a(v, w; \bar{\mu}) + a(w, v; \bar{\mu})\right), \quad \forall v, w \in X^{\rm e} \tag{13}$$

and induced norm $\|v\|_X = \sqrt{(v, v)_X}$, where $\bar{\mu} \in \mathcal{D}$ is a fixed reference parameter. We also introduce the continuity and coercivity constants of the bilinear form a as

$$\gamma_a^{\rm e}(\mu) = \sup_{v\in X^{\rm e}} \sup_{w\in X^{\rm e}} \frac{a(v, w; \mu)}{\|v\|_X \, \|w\|_X}, \qquad \forall \mu \in \mathcal{D}, \tag{14}$$

and

$$\alpha_a^{\rm e}(\mu) = \inf_{v\in X^{\rm e}} \frac{a(v, v; \mu)}{\|v\|_X^2}, \qquad \forall \mu \in \mathcal{D}, \tag{15}$$

respectively. Moreover, we assume that the bilinear form a is affine with respect to the parameter μ, i.e.

$$a(\cdot, \cdot; \mu) \equiv \sum_{q=1}^{Q_a} \vartheta_a^q(\mu)\, a^q(\cdot, \cdot), \tag{16}$$

with parameter-dependent functions $\vartheta^q(\mu)$ and parameter-independent bilinear forms a^q.

3.1.2. Truth Approximation

Since we do not have access to the exact semi-discrete solution $y^{{\rm e},k}(\mu) \in X^{\rm e}$ we replace it with a so called "truth solution" $y^k(\mu)$ that resides in a finite element approximation space $X \subset X^{\rm e}$ of very large dimension $\mathcal{N}$. Our truth approximation to (11) and (12) is then: given $\mu \in \mathcal{D}$, we evaluate

$$s(t^k; \mu) := l(y^k(\mu)), \qquad k = 1, \ldots, K, \tag{17}$$

where $y^k(\mu) \in X$ satisfies

$$m(y^{k+1}(\mu) - y^k(\mu), v) + \Delta t\, a(y^{k+\theta}(\mu), v; \mu) = \Delta t\, f(v; g(\cdot;\mu))u^{k+\theta} \tag{18}$$

for all $v \in X$ and $k = 0, 1, \ldots, K-1$, with initial condition $y^0(\mu) \equiv 0$. The continuity and coercivity constants of the bilinear form a with respect to X are given by

$$\gamma_a(\mu) = \sup_{v\in X} \sup_{w\in X} \frac{a(v, w; \mu)}{\|v\|_X \, \|w\|_X}, \qquad \forall \mu \in \mathcal{D}, \tag{19}$$

and

$$\alpha_a(\mu) = \inf_{v \in X} \frac{a(v, v; \mu)}{\|v\|_X^2}, \qquad \forall \mu \in \mathcal{D}, \tag{20}$$

respectively.

We recall that the affine parameter dependence of the bilinear and linear forms is a crucial ingredient for the computational efficiency, i.e., the offline-online decomposition, of the reduced basis method [16]. We may therefore replace the non-affine function $g(\cdot; \mu)$ in (18) by its affine coefficient-function approximation $g_M(\cdot; \mu)$ defined in (3) to obtain the *approximated* affine problem: find $y_M^k(\mu) \in X$ such that

$$m(y_M^{k+1}(\mu) - y_M^k(\mu), v) + \Delta t\, a(y_M^{k+\theta}(\mu), v; \mu) = \Delta t\, f_M(v; \mu) u^{k+\theta} \tag{21}$$

for all $v \in X$ and $k = 0, 1, \ldots, K-1$, with $y_M^0(\mu) \equiv 0$; here,

$$f_M(v; \mu) := f(v; g_M(x; \mu)) = f(v; \sum_{q=1}^{M} \omega_q(\mu) \hat{g}^q(x)) = \sum_{q=1}^{M} \omega_q(\mu) f(v; \hat{g}^q(x)) = \sum_{q=1}^{M} \omega_q(\mu) f_M^q(v), \tag{22}$$

for all $v \in X$ and $\mu \in \mathcal{D}$, where the $f_M^q(v) := f(v; \hat{g}^q(x))$, $q = 1, \ldots, M$, are parameter-independent linear forms and the $\omega_q(\mu)$, $q = 1, \ldots, M$, are calculated from (4). Note that we could now redefine (21) as our new truth approximation to obtain a problem which is affine in the parameter. We can then directly apply the standard techniques for affine problems from [27] at the cost of neglecting the error due to the empirical interpolation, see [18]. In contrast, we take the error due to the empirical interpolation explicitly into account and thus (21) only has a theoretical purpose. In fact, we stress that $y_M^k(\mu)$ is not computed at any stage in the offline phase and that our *a posteriori* error bounds derived in Section 4 measure the error of the reduced basis approximation with respect to the truth solution $y^k(\mu)$ from (18) and *not* with respect to the affine approximation $y_M^k(\mu)$ to the truth solution. We return to this discussion in Section 4.

To ensure rapid convergence of our reduced basis output approximation we introduce a dual (or adjoint) problem [22, 23]. Invoking the linear time-invariance (LTI) property, the truth approximation of the dual corresponding to the output at time t^L, $L = 1, \ldots, K$, is defined by

$$\psi_L(\cdot, t^k; \mu) = \Psi(\cdot, t^{K-L+k}; \mu), \qquad k = 1, \ldots, L, \tag{23}$$

where $\Psi^k(\mu) \equiv \Psi(\cdot, t^k; \mu) \in X$ satisfies

$$-m(v, \Psi^{k+1}(\mu) - \Psi^k(\mu)) + \Delta t\, a(v, \Psi^{k+(1-\theta)}(\mu); \mu) = 0 \tag{24}$$

for all $v \in X$ and $k = 1, \ldots, K$, with parameter-independent final condition

$$m(v, \Psi^{K+1}) = l(v) \tag{25}$$

for all $v \in X$. Note that the dual problem inherits the spatial and temporal discretization from the primal problem. Also note that the dual problem is *affine* with respect to the parameter since the source term f does not enter into the dual problem.

3.1.3. Model Problem

The welding process discussed in Section 1 shall serve as our model problem. We consider the spatial domain $\Omega := [-30, 10] \times [0, 10] \times [-10, 0]$ and a coordinate system moving with the (non-dimensional) velocity Pe of the torch in the x_1-direction. In this coordinate system, the torch is stationary at the origin and the velocity enters as a convective term in the governing equation, see Figure 2. The non-dimensionalized temperature y^{e} in the workpiece is then governed by the convection-diffusion equation (1) with $\mathrm{v} = (-\mathrm{Pe}, 0, 0)$ and the source term is given by Eq. (2), c.f. [4]. Our output of interest is the average temperature over the measurement domain Ω_{m}. According to the data in [6] we set $\mathrm{Pe} = 3.65$ for the velocity and $u \equiv 12.3$ for the control input. Our parameter is given by $\mu = (\mu_q, \kappa) = (\sigma_1, \sigma_2, \sigma_3, \kappa) \subset \mathcal{D} := \mathcal{D}_q \times [0.5, 2.0] = [1.08, 1.32]^3 \times [0.5, 2.0]$; we thus have $P = 4$ parameters. Note that the thermal diffusivity satisfies $\kappa \in [0.5, 2.0]$ which corresponds to a typical range of diffusivities for steel. We choose the time interval $I =]0, 5]$ with $K = 100$ and $\theta = 1$.

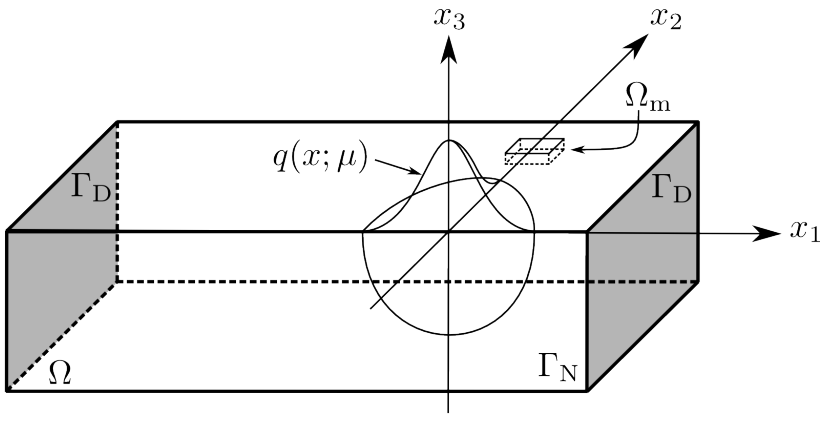

Figure 2: Sketch of the computational domain of the model problem with welding torch at the origin and the measuring point at the top side of the workpiece.

We consider the start-up of the welding process and thus set the initial condition to zero. We assume homogeneous Neumann boundary conditions on $\Gamma_{\rm N}$ and homogeneous Dirichlet boundary conditions on $\Gamma_{\rm D}$, where $\Gamma_{\rm D}$ corresponds to the inflow and outflow part of the boundary. The inflow and outflow boundaries are chosen far enough from the origin so as not to influence the temperature at the measurement location.

We next derive the weak formulation of (1) and apply the finite differences θ-method. The governing equation for the temperature $y^k(\mu) \in X$ is thus (18), where X is a linear finite element truth approximation subspace of dimension $\mathcal{N} = 23891$ with 133805 tetrahedra. The bilinear and linear forms are given by $m(w,v) = \int_\Omega wv \, \mathrm{d}x$, $a(w,v;\mu) = \kappa \int_\Omega \nabla w \cdot \nabla v \, \mathrm{d}x + \mathrm{Pe} \int_\Omega \frac{\partial}{\partial x_1} w \, v \, \mathrm{d}x$, and $f(v; q(\cdot;\mu)) = \int_\Omega v \; q(x;\mu) \, \mathrm{d}x$, with $q(x;\mu)$ given by (2); the bilinear form a admits the obvious affine representation (16) with $Q_a = 2$. We also define the inner product $(v,w)_X \equiv \int_\Omega \nabla w \cdot \nabla v \, \mathrm{d}x$ corresponding to (13) for $\bar{\kappa} = 1$; note that the parameters σ_i, $i = 1,2,3$, do not enter in the definition of the X-norm. The output of interest can be written in the form (17), i.e.,

$$s(t^k;\mu) = l(y^k(\mu)) = \frac{1}{|\Omega_{\rm m}|} \int_{\Omega_{\rm m}} y^k(\mu) \, \mathrm{d}x, \qquad k = 1, \ldots, K, \tag{26}$$

where $\Omega_{\rm m} = [-0.25, 0.25] \times [1.5, 2] \times [-0.1, 0]$. In Figure 3 (a) and (b) we show the temperature variation over the workpiece at the discrete timesteps $k = 10$ and $k = 100$, respectively; note that the plot at $k = 100$ is close to the steady-state solution.

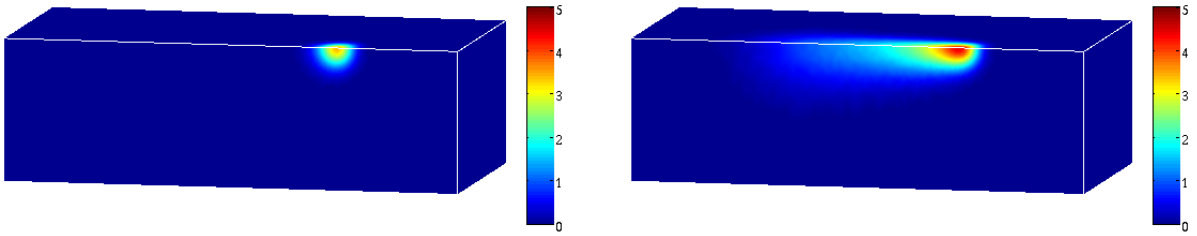

(a) $k = 10$ (b) $k = 100$

Figure 3: Temperature distribution on the surface of the workpiece for $\mu = (1.2, 1.2, 1.2, 0.5)$ at the discrete times (a) $t = t^{10} = 0.5$ and (b) $t = t^{100} = 5$.

3.2. Reduced Basis Approximation

We suppose that we are given the nested Lagrangian reduced basis spaces

$$X_{N^{\rm pr}}^{\rm pr} = \mathrm{span}\{\zeta^{{\rm pr},n}(x), \; 1 \le n \le N^{\rm pr}\}, \quad 1 \le N^{\rm pr} \le N_{\rm max}^{\rm pr}, \tag{27}$$

and

$$X^{\rm du}_{N^{\rm du}} = \text{span}\{\zeta^{{\rm du},n}(x),\ 1 \le n \le N^{\rm du}\}, \quad 1 \le N^{\rm du} \le N^{\rm du}_{\rm max}, \tag{28}$$

where the $\zeta^{{\rm pr},n},\ 1 \le n \le N^{\rm pr}$, and the the $\zeta^{{\rm du},n},\ 1 \le n \le N^{\rm du}$, are mutually $(\cdot,\cdot)_X$-orthogonal basis functions. In general, we have $N^{\rm pr} \neq N^{\rm du}$. We comment on the POD/Greedy algorithm for constructing the basis functions in Section 5.

Our reduced basis approximation $y^k_{M,N^{\rm pr}}(\mu)$ to $y^k(\mu)$ is obtained by a standard Galerkin projection: given $\mu \in \mathcal{D}$, $y^k_{M,N^{\rm pr}}(\mu) \in X^{\rm pr}_{N^{\rm pr}}$ satisfies

$$m(y^{k+1}_{M,N^{\rm pr}}(\mu) - y^k_{M,N^{\rm pr}}(\mu), v) + \Delta t\, a(y^{k+\theta}_{M,N^{\rm pr}}(\mu), v; \mu) = \Delta t\, f_M(v;\mu) u^{k+\theta} \tag{29}$$

for all $v \in X^{\rm pr}_{N^{\rm pr}}$ and $k = 0, 1, \ldots, K-1$, with initial condition $y^0_{M,N^{\rm pr}}(\mu) = 0$.

Similarly, we obtain the reduced basis approximation $\Psi^k_{N^{\rm du}}(\mu) \in X^{\rm du}_{N^{\rm du}}$ to $\Psi^k(\mu) \in X$ as the solution of

$$-m(v, \Psi^{k+1}_{N^{\rm du}}(\mu) - \Psi^k_{N^{\rm du}}(\mu)) + \Delta t\, a(v, \Psi^{k+(1-\theta)}_{N^{\rm du}}(\mu); \mu) = 0 \tag{30}$$

for all $v \in X^{\rm du}_{N^{\rm du}}$ and $k = 1, \ldots, K$, with final condition

$$m(v, \Psi^{K+1}_{N^{\rm du}}) = l(v) \tag{31}$$

for all $v \in X^{\rm du}_{N^{\rm du}}$.

Let $N = (N^{\rm pr}, N^{\rm du})$ be a multi-index indicating the reduced basis dimension of the primal and dual problem, respectively. The reduced basis approximation of the output can then be evaluated as

$$s^k_{M,N}(\mu) = l(y^k_{M,N^{\rm pr}}(\mu)) + \Delta t \sum_{k'=1}^{k} r^{y,k'}_{N^{\rm pr}}(\Psi^{K-k+k'+(1-\theta)}_{N^{\rm du}}(\mu); \mu), \tag{32}$$

for $k = 1, \ldots, K$; here, the residual of the primal problem is defined as

$$r^{y,k}_{N^{\rm pr}}(v;\mu) := f_M(v;\mu) u^{k-1+\theta} - a(y^{k-1+\theta}_{M,N^{\rm pr}}(\mu), v; \mu) - \frac{1}{\Delta t} m(y^k_{M,N^{\rm pr}}(\mu) - y^{k-1}_{M,N^{\rm pr}}(\mu), v), \tag{33}$$

with $k = 1, \ldots, K$ for all $v \in X$. We may also obtain a primal-only reduced basis output approximation from

$$\tilde{s}^k_{M,N^{\rm pr}}(\mu) = l(y^k_{M,N^{\rm pr}}(\mu)), \tag{34}$$

$k = 1, \ldots, K$. Note that we do not require the dual problem to evaluate $\tilde{s}^k_{M,N^{\rm pr}}(\mu)$. We shall compare the performance of both output approximations in Section 6.

3.3. Computational Procedure

We briefly summarize the well-known offline-online decomposition and concentrate on the contributions due to the EIM; see e.g. [14, 25] for elliptic, [26, 27] for parabolic, and [16, 17, 19, 20] for non-affine and certain classes of nonlinear problems. We first express $y^k_{M,N^{\rm pr}}(\mu)$ as $y^k_{M,N^{\rm pr}}(\mu) = \sum_{i=1}^{N^{\rm pr}} y^k_{M,N^{\rm pr}\,i}(\mu)\zeta^{{\rm pr},i}$ and choose as test functions $v = \zeta^{{\rm pr},i}(x),\ 1 \le i \le N^{\rm pr}$ in (29). It then follows that $\underline{y}^k_{M,N^{\rm pr}}(\mu) = [y^k_{M,N^{\rm pr}\,1}(\mu), \ldots, y^k_{M,N^{\rm pr}\,N^{\rm pr}}(\mu)]^{\rm T} \in \mathbb{R}^{N^{\rm pr}}$ satisfies

$$\left(M^{\rm pr}_N + \theta\Delta t\, A^{\rm pr}_N(\mu)\right)^{\rm T} \underline{y}^{k+1}_{M,N^{\rm pr}}(\mu) = \left(M^{\rm pr}_N - (1-\theta)\,\Delta t\, A^{\rm pr}_N(\mu)\right)^{\rm T} \underline{y}^k_{M,N^{\rm pr}}(\mu) + \Delta t\,\left((1-\theta)\,u^k + \theta u^{k+1}\right) F^{\rm pr}_M(\mu), \quad (35)$$

for $k = 0, 1, \ldots, K-1$, with initial condition $\underline{y}^0_{M,N^{\rm pr}}(\mu) = \underline{0}$. Here, $A^{\rm pr}_N(\mu)$ and $M^{\rm pr}_N$ are $N^{\rm pr} \times N^{\rm pr}$ matrices with entries $A^{\rm pr}_{N\,ij}(\mu) = a(\zeta^{{\rm pr},i}, \zeta^{{\rm pr},j}; \mu),\ 1 \le i, j \le N^{\rm pr}$, and $M^{\rm pr}_{N\,ij} = m(\zeta^{{\rm pr},i}, \zeta^{{\rm pr},j}),\ 1 \le i, j \le N^{\rm pr}$, respectively; and the vector $F^{\rm pr}_M(\mu) \in \mathbb{R}^{N^{\rm pr}}$ has entries $F^{\rm pr}_{M\,j}(\mu) = f_M(\zeta^{{\rm pr},j}; \mu), 1 \le j \le N^{\rm pr}$. Invoking the affine parameter dependence (16) we obtain $A^{\rm pr}_N(\mu) = \sum_{q=1}^{Q_a} \vartheta^q_a(\mu) A^{{\rm pr},q}_N$, where the parameter independent matrices $A^{{\rm pr},q}_N \in \mathbb{R}^{N^{\rm pr}\times N^{\rm pr}},\ 1 \le q \le Q_a$, have entries $A^{{\rm pr},q}_{N\,ij} = a^q(\zeta^{{\rm pr},i}, \zeta^{{\rm pr},j}),\ 1 \le i, j \le N^{\rm pr},\ 1 \le q \le Q_a$.

We note that the approximation $g_M(\cdot;\mu)$ to the non-affine function $g(\cdot;\mu)$ defined in (3) is independent of the truth approximation and thus generated in advance following the standard EIM procedure in Section 2.1. It then directly follows from (22) that we can express $F^{\rm pr}_M(\mu)$ as

$$F^{\rm pr}_M(\mu) = \sum_{q=1}^{M} \omega_q(\mu) F^{{\rm pr},q}_M, \quad (36)$$

where the parameter independent vectors $F^{{\rm pr},q}_M \in \mathbb{R}^{N^{\rm pr}},\ 1 \le q \le M$, are given by $F^{{\rm pr},q}_{M\,j} = f^q_M(\zeta^{{\rm pr},j}) = f(\zeta^{{\rm pr},j}; \hat{g}^q(x)),\ 1 \le j \le N^{\rm pr},\ 1 \le q \le M$, and the $\omega_q(\mu),\ 1 \le q \le M$, are calculated from (4). The computational procedure for the dual problem and the output approximation directly follows from the primal problem and is therefore omitted [26, 27].

The offline-online decomposition is now clear. In the offline stage — performed only once — we compute (say, for the primal problem) the parameter-independent quantities $A^{{\rm pr},q}_N$, $M^{\rm pr}_N$, and $F^{{\rm pr},q}_M$; the computational cost clearly depends on $\mathcal{N}$. In the online stage — performed many times, for each new parameter value μ — we first assemble (again, for the primal problem) the parameter-dependent matrix $A^{\rm pr}_N(\mu)$ and vector $F^{\rm pr}_M(\mu)$ at cost $\mathcal{O}(Q_a(N^{\rm pr})^2 + M^2 + MN^{\rm pr})$. We then solve (35) at cost $\mathcal{O}((N^{\rm pr})^3 + K(N^{\rm pr})^2)$ and evaluate the output approximation (32) at

time t^k at cost $\mathcal{O}(kN^{\rm pr}N^{\rm du})$; note that the evaluation of the output for all K timesteps has a cost of $\mathcal{O}(K^2N^{\rm pr}N^{\rm du})$ due to the residual correction term. Evaluating the primal-only reduced basis output approximation (34) at all timesteps costs only $\mathcal{O}(KN^{\rm pr})$. The online stage is thus independent of the truth finite element dimension $\mathcal{N}$.

4. *A Posteriori* Error Estimation

In this section we develop rigorous *a posteriori* error bounds for the reduced basis approximation of the state and output. The new ingredients are (*i*) the combination of the rigorous error bounds for the EIM of Section 2 with the "standard" affine reduced basis error bounds, and (*ii*) the development of primal-dual formulations for non-affine parabolic problems. We recall that non-rigorous error bounds have been developed for elliptic and parabolic problems in [17, 19] and [20], respectively; and that primal-dual formulations for *affine* parabolic problems have been proposed in [27]. Furthermore, we refer the interested reader to [16] for *a priori* convergence results of non-affine problems.

4.1. Preliminaries

To begin, we assume that we are given a positive lower bound for the coercivity constant $\alpha_a(\mu)$: $\alpha_a^{\rm LB}(\mu) : \mathcal{D} \rightarrow \mathbb{R}_+$ satisfies

$$\alpha_a(\mu) \geq \alpha_a^{\rm LB}(\mu) \geq \alpha_a^0 > 0, \quad \forall\, \mu \in \mathcal{D}. \tag{37}$$

This bound can be calculated using the Successive Constraint Method (SCM) [32]; however, simpler recipes often suffice [25, 33]. We next introduce the dual norm of the primal residual (33), given by

$$\left\| r_{N^{\rm pr}}^{y,k}(\cdot;\mu) \right\|_{X^*} = \sup_{v \in X} \frac{r_{N^{\rm pr}}^{y,k}(v;\mu)}{\|v\|_X}, \quad 1 \leq k \leq K, \tag{38}$$

and the dual norm of the dual residual

$$\left\| r_{N^{\rm du}}^{\Psi,k}(\cdot;\mu) \right\|_{X^*} = \sup_{v \in X} \frac{r_{N^{\rm du}}^{\Psi,k}(v;\mu)}{\|v\|_X}, \quad 1 \leq k \leq K, \tag{39}$$

where

$$r_{N^{\rm du}}^{\Psi,k}(v;\mu) := -a(v, \Psi_{N^{\rm du}}^{k+(1-\theta)}(\mu);\mu) + \frac{1}{\Delta t} m(v, \Psi_{N^{\rm du}}^{k+1}(\mu) - \Psi_{N^{\rm du}}^{k}(\mu)), \tag{40}$$

for $v \in X$, $1 \leq k \leq K$. Finally, the spatio-temporal energy norm for the primal problem is defined as

$$\left|\!\left|\!\left| v^k \right|\!\right|\!\right|_\mu^{\text{pr}} := \left(m(v^k, v^k) + \Delta t \sum_{k'=1}^{k} a(v^{k'-1+\theta}, v^{k'-1+\theta}; \mu) \right)^{\frac{1}{2}}, \tag{41}$$

and for the dual problem as

$$\left|\!\left|\!\left| v^k \right|\!\right|\!\right|_\mu^{\text{du}} := \left(m(v^k, v^k) + \Delta t \sum_{k'=k}^{K} a(v^{k+(1-\theta)}, v^{k+(1-\theta)}; \mu) \right)^{\frac{1}{2}}. \tag{42}$$

4.2. Primal Variable

We first revisit our discussion related to the truth formulation (18) and its affine approximation (21). Assuming we are interested in the error between the reduced basis approximation, $y^k_{M,N^{\text{pr}}}(\mu)$, and the affine approximation to the truth, $y^k_M(\mu)$, we can directly apply the result from [27]. Indeed, the error, $y^k_M(\mu) - y^k_{M,N^{\text{pr}}}(\mu)$, satisfies

$$\left|\!\left|\!\left| y^k_M(\mu) - y^k_{M,N^{\text{pr}}}(\mu) \right|\!\right|\!\right|_\mu^{\text{pr}} \leq \Delta^{y_M,k}_{N^{\text{pr}}}(\mu), \quad \forall \mu \in \mathcal{D},\ \forall k = 1, \ldots, K, \tag{43}$$

where the error bound is given by

$$\Delta^{y_M,k}_{N^{\text{pr}}}(\mu) := \left(\frac{\Delta t}{\alpha_a^{\text{LB}}(\mu)} \sum_{k'=1}^{k} \left\| r^{y,k'}_{N^{\text{pr}}}(\cdot; \mu) \right\|^2_{X^*} \right)^{\frac{1}{2}}. \tag{44}$$

Although this approach is appealing due to its simplicity, the error bound (44) *does not* account for the error due to the empirical interpolation of the non-affine terms. Our goal is to incorporate the interpolation error into the bound formulation and thus provide a rigorous upper bound for the error between the reduced basis, $y^k_{M,N^{\text{pr}}}(\mu)$, and the truth approximation, $y^k(\mu)$. However, we shall use the bound defined in (44) for notational convenience and to show the analogy between the affine and non-affine error bound formulations.

We are now ready to state

Proposition 1. *Let $\mathcal{P} = (p, \Phi)$ be a multi-index with a positive integer p and a finite subset Φ of $\mathcal{D}$. Then the error*

$$e^{y,k}_{M,N^{\text{pr}}}(\mu) \equiv y^k(\mu) - y^k_{M,N^{\text{pr}}}(\mu) \tag{45}$$

of the reduced basis solution $y^k_{M,N^{\text{pr}}}(\mu)$ with respect to the truth solution $y^k(\mu)$ satisfies

$$\left|\!\left|\!\left| e^{y,k}_{M,N^{\text{pr}}}(\mu) \right|\!\right|\!\right|_\mu^{\text{pr}} \leq \Delta^{y,k}_{M,N^{\text{pr}},\mathcal{P}}(\mu), \qquad \forall \mu \in \mathcal{D},\ \forall k = 1, \ldots, K, \tag{46}$$

where the error bound $\Delta^{y,k}_{M,N^{\rm pr},\mathcal{P}}(\mu)$ *is defined as*

$$\Delta^{y,k}_{M,N^{\rm pr},\mathcal{P}}(\mu) := \left(2\left(\Delta^{y_M,k}_{N^{\rm pr}}(\mu)\right)^2 + \frac{2\Delta t}{\alpha_a^{\rm LB}(\mu)}\left(\delta^g_{M,p,\Phi}\,\|f(\cdot;1)\|_{X^*}\right)^2 \sum_{k'=1}^{k}\left(u^{k-1+\theta}\right)^2\right)^{\frac{1}{2}}, \tag{47}$$

$\Delta^{y_M,k}_{N^{\rm pr}}(\mu)$ *is defined in (44), and* $\|f(\cdot;1)\|_{X^*} := \sup_{v\in X}\frac{f(v;1)}{\|v\|_X}$.

We note that the error bound (47) consists of two terms: the first term contains the error bound defined in (44) and thus represents the contribution due to the affine terms; the second term depends on the estimator $\delta^g_{M,p,\Phi}$ for the interpolation error, and thus accounts for the error due to the non-affine function interpolation.

Proof. The proof is an extension of the one presented in [27] for affine problems with the added complexity due to error in the function interpolation. Following the same steps, we obtain

$$\begin{aligned} m(e^{y,k}_{M,N^{\rm pr}}, e^{y,k}_{M,N^{\rm pr}}) - m(e^{y,k-1}_{M,N^{\rm pr}}, e^{y,k-1}_{M,N^{\rm pr}}) + 2\Delta t\, a(e^{y,k-1+\theta}_{M,N^{\rm pr}}, e^{y,k-1+\theta}_{M,N^{\rm pr}};\mu) \\ \leq 2\Delta t\, r^{y,k}_{N^{\rm pr}}(e^{y,k-1+\theta}_{M,N^{\rm pr}};\mu) + 2\Delta t\, f(e^{y,k-1+\theta}_{M,N^{\rm pr}}, g(\mu) - g_M(\mu))u^{k-1+\theta}. \end{aligned} \tag{48}$$

The new ingredient is the non-affine contribution on the right hand side. Using Young's inequality, the first term on the right hand side can be bounded by

$$r^{y,k}_{N^{\rm pr}}(e^{y,k-1+\theta}_{M,N^{\rm pr}};\mu) \leq \frac{1}{2}\left(\frac{2}{\alpha_a^{\rm LB}(\mu)}\left\|r^{y,k}_{N^{\rm pr}}(\cdot;\mu)\right\|^2_{X^*} + \frac{\alpha_a^{\rm LB}(\mu)}{2}\left\|e^{y,k-1+\theta}_{M,N^{\rm pr}}\right\|^2_X\right). \tag{49}$$

We now use the EIM rigorous bound result (8), (9), and Young's inequality to bound the second term on the right hand side by

$$\begin{aligned} f(e^{y,k-1+\theta}_{M,N^{\rm pr}}, g(\mu) - g_M(\mu))u^{k-1+\theta} \\ \leq \frac{1}{2}\left(\frac{\alpha_a^{\rm LB}(\mu)}{2}\left\|e^{y,k-1+\theta}_{M,N^{\rm pr}}\right\|^2_X + \frac{2}{\alpha_a^{\rm LB}(\mu)}\left(\delta^g_{M,p,\Phi}\,\|f(\cdot;1)\|_{X^*}\,u^{k-1+\theta}\right)^2\right). \end{aligned} \tag{50}$$

The desired result then directly follows from (48), (49), (50), the coercivity of a and (37) after summing from $k'=1$ to k.

□

4.3. Dual Variable

Since the dual problem is affinely parameter dependent, the results from [27] directly apply: the error

$$e^{\Psi,k}_{N^{\rm du}}(\mu) \equiv \Psi^k(\mu) - \Psi^k_{N^{\rm du}}(\mu) \tag{51}$$

in the dual state satisfies

$$\left|\left|\left| e^{\Psi,k}_{N^{\rm du}}(\mu) \right|\right|\right|^{\rm du}_{\mu} \le \Delta^{\Psi,k}_{N^{\rm du}}(\mu) \qquad \forall \mu \in \mathcal{D},\ \forall k = 1, \ldots, K, \tag{52}$$

where the dual state error bound is given by

$$\Delta^{\Psi,k}_{N^{\rm du}}(\mu) := \left(\frac{\Delta t}{\alpha^{\rm LB}_a(\mu)} \sum_{k'=k}^{K} \left\| r^{\Psi,k'}_{N^{\rm du}}(\cdot;\mu) \right\|^2_{X^*} \right)^{\frac{1}{2}}. \tag{53}$$

4.4. Output Bounds

Finally, the error bound for the output approximation is given in the following proposition. We provide the proof in Appendix A.

Proposition 2. *Let $\mathcal{P} = (p, \Phi)$ be a multi-index with a positive integer p and a finite subset Φ of $\mathcal{D}$. The error between the truth output $s^k(\mu)$ and its reduced basis approximation $s^k_{M,N}(\mu)$ satisfies*

$$\left| s^k(\mu) - s^k_{M,N}(\mu) \right| \le \Delta^{s,k}_{M,N,\mathcal{P}}(\mu) \qquad \forall \mu \in \mathcal{D},\ \forall k = 1, \ldots, K, \tag{54}$$

with the primal-dual output error bound

$$\begin{aligned} \Delta^{s,k}_{M,N,\mathcal{P}}(\mu) := {} & \Delta^{y_M,k}_{N^{\rm pr}}(\mu)\ \Delta^{\Psi,K-k+1}_{N^{\rm du}}(\mu) \\ & + \delta^g_{M,p,\Phi}\ \Delta^{\Psi,K-k+1}_{N^{\rm du}}(\mu)\ \|f(\cdot;1)\|_{X^*} \left(\frac{\Delta t}{\alpha^{\rm LB}_a(\mu)} \sum_{k'=1}^{k} \left(u^{k'-1+\theta} \right)^2 \right)^{\frac{1}{2}} \\ & + \Delta t\, \delta^g_{M,p,\Phi} \sum_{k'=1}^{k} \left| f(\Psi^{K-k+k'+(1-\theta)}_{N^{\rm du}}(\mu);1)\ u^{k'-1+\theta} \right|, \end{aligned} \tag{55}$$

where $\Delta^{y_M,k}_{N^{\rm pr}}(\mu)$ and $\Delta^{\Psi,k}_{N^{\rm du}}(\mu)$ are defined in (44) and (53), respectively.

We also introduce a primal-only reduced basis output approximation and corresponding error bound which shall serve as a comparison for the primal-dual formulation.

Proposition 3. *Let $\mathcal{P} = (p, \Phi)$ be a multi-index with a positive integer p and a finite subset Φ of $\mathcal{D}$. The error between the truth output $s^k(\mu)$ and its primal-only reduced basis approximation $\tilde{s}^k_{M,N^{\rm pr}}(\mu)$ satisfies*

$$\left| s^k(\mu) - \tilde{s}^k_{M,N^{\rm pr}}(\mu) \right| \le \tilde{\Delta}^{s,k}_{M,N^{\rm pr},\mathcal{P}}(\mu) \qquad \forall \mu \in \mathcal{D},\ \forall k = 1, \ldots, K, \tag{56}$$

with the primal-only output error bound

$$\tilde{\Delta}^{s,k}_{M,N^{\rm pr},\mathcal{P}}(\mu) := \sup_{v \in X} \frac{l(v)}{\|v\|_{L^2(\Omega)}} \Delta^{y,k}_{M,N^{\rm pr},\mathcal{P}}(\mu). \tag{57}$$

Proof. From the definition of the primal-only output we obtain

$$\left|s^k(\mu) - \tilde{s}^k_{M,N^{\rm pr}}(\mu)\right| = \left|l(e^{y,k}_{M,N^{\rm pr}}(\mu))\right| = \sup_{v\in X} \frac{l(v)}{\|v\|_{L^2(\Omega)}} \left\|e^{y,k}_{M,N^{\rm pr}}(\mu)\right\|_{L^2(\Omega)}. \tag{58}$$

The result directly follows since

$$\left\|e^{y,k}_{M,N^{\rm pr}}(\mu)\right\|_{L^2(\Omega)} = \left(m(e^{y,k}_{M,N^{\rm pr}}(\mu), e^{y,k}_{M,N^{\rm pr}}(\mu))\right)^{\frac{1}{2}} \leq \left|\left|\left|e^{y,k}_{M,N^{\rm pr}}(\mu)\right|\right|\right|^{\rm pr}_{\mu}. \tag{59}$$

for all $\mu \in \mathcal{D}$. □

At this point, we make several comments from a theoretical point of view. First, similar to the error bound for the primal variable, the output error bound (55) consists of several terms: the first term represents the usual primal-dual contribution to the error bound. If the problem becomes affine, i.e., we redefine the affine approximation to the truth finite element approximation given by (21) to be our new "truth" the error bound then simplifies to the one proposed for affine problems in [27]: the interpolation error bound $\delta^g_{M,p,\Phi}$ vanishes and only the primal-dual contribution in the first term, $\Delta^{y_M,k}_{N^{\rm pr}}(\mu)\ \Delta^{\Psi,K-k+1}_{N^{\rm du}}(\mu)$, remains. However, for non-affine problems we obtain two additional terms which account for the error due to the function approximation.

Second, the goal of the primal-dual formulation is to obtain a corrected output functional which is superconvergent, i.e., the output bound is the product of the primal error bound and the dual error bound [22, 23, 24]. The second term of the output error bound (55) also shows this square effect since the error bound of the dual state is multiplied with the EIM error bound. The last term, on the other side, only contains the EIM error bound $\delta^g_{M,p,\Phi}$. We thus need to choose M large enough — and thus guarantee that $\delta^g_{M,p,\Phi}$ is small enough — so that the last term does not spoil the superconvergence of the overall output error bound. We recall that the last term does not appear if the problem is affine [25, 26, 27].

Third, we observe that the primal-only output error bound is not superconvergent. We thus expect a much slower convergence of the output bound for the primal-only formulation.

4.5. Computational Procedure

The offline-online computational procedures for the calculation of the error bounds $\Delta^{y,k}_{M,N^{\rm pr},\mathcal{P}}(\mu)$, $\tilde{\Delta}^{s,k}_{M,N^{\rm pr},\mathcal{P}}(\mu)$ and $\Delta^{s,k}_{M,N,\mathcal{P}}(\mu)$ are a direct extension of the procedures described in [27, 20]. We therefore omit the details and only summarize the computational costs involved in the online stage.

We recall that the EIM *a posteriori* error bound $\delta^g_{M,p,\Phi}$ is evaluated offline and does not require any online calculations. In the online stage the computational cost to evaluate $\Delta^{y,k}_{M,N^{\rm pr},\mathcal{P}}(\mu)$ and $\tilde{\Delta}^{s,k}_{M,N^{\rm pr},\mathcal{P}}(\mu)$ for all K is thus $\mathcal{O}(K(N^{\rm pr}MQ_a+(N^{\rm pr})^2Q_a^2))$, while the computational cost to evaluate the primal-dual output bound $\Delta^{s,k}_{M,N,\mathcal{P}}(\mu)$ is $\mathcal{O}(K(N^{\rm pr}MQ_a + (N^{\rm pr})^2Q_a^2 + (N^{\rm du})^2Q_a^2))$.

5. Sampling Procedure

We employ the POD/Greedy procedure introduced in [34], also see [35], to construct the primal and dual reduced basis space. We briefly summarize the procedure for the primal problem: we first choose an arbitrary parameter value $\mu_1 \in \mathcal{D}$ and set $S_0 = \{0\}$, $X_0 = \{0\}$, $N^{\rm pr} = 0$. Then, for $1 \le N^{\rm pr} \le N^{\rm pr}_{\rm max}$, we first set $S_{N^{\rm pr}} = S_{N^{\rm pr}-1} \cup \{\mu_{N^{\rm pr}}\}$ and compute the projection error $e^{y,k}_{N^{\rm pr},{\rm proj}}(\mu_{N^{\rm pr}}) = y^k(\mu_{N^{\rm pr}}) - y^k_{\rm proj}(\mu_{N^{\rm pr}})$, $k = 1,\ldots,K$, where $y^k_{\rm proj}(\mu_{N^{\rm pr}})$ is the X-orthogonal projection of the truth solution $y^k(\mu_{N^{\rm pr}})$ onto the reduced basis space $X_{N^{\rm pr}}$. We then expand the reduced basis space by the largest POD mode of the time history of $\{e^{y,k}_{N^{\rm pr},{\rm proj}}(\mu_{N^{\rm pr}}) \mid 1 \le k \le K\}$ which we compute using the method of snapshots [36]. Finally, we choose the next parameter value from $\mu_{N^{\rm pr}+1} = \arg\max_{\mu\in\Xi_{\rm train}} \Delta^{y,K}_{M,N^{\rm pr}}(\mu)/|||y^K_{M,N^{\rm pr}}(\mu)|||^{\rm pr}_\mu$, i.e. we perform a greedy search over $\Xi_{\rm train}$ for the largest relative *a posteriori* state error bound at the final time. Here $\Xi_{\rm train} \subset \mathcal{D}$ denotes a finite but suitably large parameter train sample.

We note that $\Delta^{y,K}_{M,N^{\rm pr}}(\mu)$ also contains the contribution due to the non-affine function approximation. It is thus essential to set $M = M_{\rm max}$ during the greedy procedure so that the non-affine contribution does not spoil the greedy search; see also the discussion related to Figure 4 in the next section.

6. Numerical Results

We now present numerical results for our model problem introduced in Section 3.1.3. We recall the inner product $(v,w)_X \equiv \int_\Omega \nabla w \cdot \nabla v \, {\rm d}x$; we may hence choose $\alpha_{\rm LB}(\mu) = \kappa$ in (37). The generation of the EIM approximation of the non-affine source term and the numerical results are discussed in Section 2.3. We first choose a random parameter sample $\Xi_{\rm train} \subset \mathcal{D}$ with 1000 elements to construct the primal and dual reduced basis spaces $X^{\rm pr}_{N^{\rm pr}}$ and $X^{\rm du}_{N^{\rm du}}$ according to the POD/Greedy sampling procedure in Section 5, respectively. For the numerical tests we use a random parameter test sample $\Xi_{\rm test} \subset \mathcal{D}$ with 60 elements.

In Figure 4 we plot, as a function of $N^{\rm pr}$ and M, the maximum relative state error bound $\Delta^{y,\max,\rm rel}_{M,N^{\rm pr},\mathcal{P}} = \max_{\mu\in\Xi_{\rm test}} \Delta^{y,K}_{M,N^{\rm pr},\mathcal{P}}(\mu)/\left|\!\left|\!\left| y^K(\mu)\right|\!\right|\!\right|^{\rm pr}_\mu$ of the primal problem at the final time step t^K. For the interpolation error bound we used $p = 5$ and $\Phi = \Phi_2$. We observe that the reduced basis approximation converges quite rapidly. We also note that the curves for fixed M stagnate at some point and that the curves level off at smaller values as M increases: for fixed M the EIM error bound will ultimately dominate for large $N^{\rm pr}$; increasing M renders the coefficient function approximation more accurate, which in turn leads to a drop in the error. The separation points of the $N^{\rm pr}$-M-convergence curves reflect a balanced contribution of both error bound terms in (47); neither $N^{\rm pr}$ nor M limit the convergence of the reduced basis approximation.

We recall that the bound (47) is a provable rigorous upper bound for the reduced basis error for all values of $N^{\rm pr}$ and M. If we were to employ the non-rigorous error bound for the EIM, however, we obtain an upper bound for the reduced basis error only if we can guarantee that the error bound contribution due to the non-affine function interpolation is much smaller than the contribution due to the affine terms. A conservative choice for $N^{\rm pr}$ and M should therefore be based on the convergence curves in Figure 4.

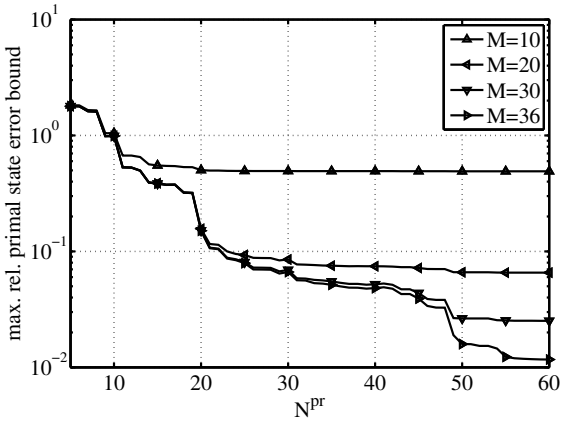

Figure 4: Numerical results for the reduced basis method: maximum relative primal state error bound $\Delta^{y,\max,\rm rel}_{M,N^{\rm pr},\mathcal{P}}$ as a function of $N^{\rm pr}$ for $M = 10, 20, 30, 36$, $p = 5$, and $\Phi = \Phi_2$.

In Table 2 we present, as a function of $N^{\rm pr}$ and M, the maximum relative truth error $\varepsilon^{y,\max,\rm rel}_{M,N^{\rm pr}}$, the maximum relative error bound $\Delta^{y,\max,\rm rel}_{M,N^{\rm pr},\mathcal{P}}$, and the average effectivity $\eta^{y,\rm ave}_{M,N^{\rm pr},\mathcal{P}}$; here, $\varepsilon^{y,\max,\rm rel}_{M,N^{\rm pr}}$ is the maximum over $\Xi_{\rm test}$ of $\varepsilon^{y,K}_{M,N^{\rm pr}}(\mu)/\left|\!\left|\!\left| y^K(\mu)\right|\!\right|\!\right|^{\rm pr}_\mu$, and $\eta^{y,\rm ave}_{M,N^{\rm pr},\mathcal{P}}$ is the average over $\Xi_{\rm test}$ of $\Delta^{y,K}_{M,N^{\rm pr},\mathcal{P}}(\mu)/\varepsilon^{y,K}_{M,N^{\rm pr}}(\mu)$. Note that the tabulated $(N^{\rm pr}, M)$ values correspond roughly to the sep-

aration points of the N^{pr}-M-convergence curves. We observe that the effectivities are larger than but close to 1; we obtain provable rigorous and sharp upper bounds for the true error.

N^{pr}	M	$\varepsilon^{y,\mathrm{max,rel}}_{M,N^{\mathrm{pr}}}$	$\Delta^{y,\mathrm{max,rel}}_{M,N^{\mathrm{pr}},\mathcal{P}}$	$\eta^{y,\mathrm{ave}}_{M,N^{\mathrm{pr}},\mathcal{P}}$
10	10	1.76E-01	1.05E+00	5.95
20	20	2.91E-02	1.57E-01	5.79
40	30	1.31E-02	5.21E-02	5.33
60	36	2.66E-03	1.17E-02	5.80

Table 2: Reduced basis approximation of the primal state: maximum relative truth error $\varepsilon^{y,\mathrm{max,rel}}_{M,N^{\mathrm{pr}}}$, maximum relative error bound $\Delta^{y,\mathrm{max,rel}}_{M,N^{\mathrm{pr}},\mathcal{P}}$ and average effectivity $\eta^{y,\mathrm{ave}}_{M,N^{\mathrm{pr}},\mathcal{P}}$ as a function of M and N^{pr}. The values of the error bound refer to $p = 5$ and $\Phi = \Phi_2$.

The corresponding results for the dual problem are presented in Table 3. Since the dual problem only depends on one parameter, i.e., the diffusivity, we observe a slightly faster convergence of the error and the error bound than for the primal problem. The effectivities are close to 1 for all values of N^{du}, again confirming the sharpness of the error bound

N^{du}	$\varepsilon^{\Psi,\mathrm{max,rel}}_{N^{\mathrm{du}}}$	$\Delta^{\Psi,\mathrm{max,rel}}_{N^{\mathrm{du}}}$	$\eta^{\Psi,\mathrm{ave}}_{N^{\mathrm{du}}}$
10	5.06E-02	1.70E-01	3.54
20	9.25E-03	2.98E-02	3.06
40	6.24E-04	3.38E-03	4.99
60	6.19E-05	1.65E-04	3.51

Table 3: Reduced basis approximation of the dual state: maximum relative truth error $\varepsilon^{\Psi,\mathrm{max,rel}}_{N^{\mathrm{du}}}$, maximum relative error bound $\Delta^{\Psi,\mathrm{max,rel}}_{N^{\mathrm{du}}}$ and average effectivity $\eta^{\Psi,\mathrm{ave}}_{N^{\mathrm{du}}}$ as a function of N^{du}. Here, $\varepsilon^{\Psi,\mathrm{max,rel}}_{N^{\mathrm{du}}}$ and $\Delta^{\Psi,\mathrm{max,rel}}_{N^{\mathrm{du}}}$ are the maxima over Ξ_{test} of $\varepsilon^{\Psi,1}_{N^{\mathrm{du}}}(\mu)/\left|\!\left|\!\left|\Psi^1(\mu)\right|\!\right|\!\right|^{\mathrm{du}}_{\mu}$ and $\Delta^{\Psi,1}_{N^{\mathrm{du}}}/\left|\!\left|\!\left|\Psi^1(\mu)\right|\!\right|\!\right|^{\mathrm{du}}_{\mu}$, respectively; and $\eta^{\Psi,\mathrm{ave}}_{N^{\mathrm{du}}}$ is the average over Ξ_{test} of $\Delta^{\Psi,1}_{N^{\mathrm{du}}}(\mu)/\varepsilon^{\Psi,1}_{N^{\mathrm{du}}}(\mu)$.

We next turn to the output error bound and present in Figure 5 (a) and (b) the maximum relative primal-dual output error bound, $\Delta^{s,\mathrm{max,rel}}_{M,N,\mathcal{P}} = \max_{\mu\in\Xi_{\mathrm{test}}} \Delta^{s,K}_{M,N,\mathcal{P}}(\mu)/|s^K(\mu)|$, at the final time step t^K as a function of N^{pr} and N^{du} for $p = 5$, $\Phi = \Phi_2$ and $M = 20$ and $M = 36$, respectively. We first observe that the convergence curves for $M = 20$ only reach an accuracy of approximately 2×10^{-3}. At this point the interpolation error bound, i.e., the last term in (55),

dominates the primal-dual output error bound. Thus, increasing N^{pr} or N^{du} has no effect on the convergence of the output bound anymore. This is in contrast to the results for affine problems, where only the first term in (55) is present and the convergence curves thus keep decreasing without reaching a plateau. If we increase M to 36 the error bound decreases further and the stagnation of the convergence curves is not visible anymore. We note that this plateau effect is important in choosing an efficient combination of N^{pr} vs. N^{du} vs. M. As a general guideline, M should be large enough such that the interpolation error is small enough for the last term in (55) to have the same order of magnitude as the first term. Subsequently, N^{pr} and N^{du} can be chosen so as to minimize the computational cost involved. The actual values of N^{pr}, N^{du}, and M required to satisfy these goals, however, are strongly problem dependent.

We also note that the error bound decreases for fixed N^{du} as N^{pr} increases and vice versa. We can obtain a specific desired accuracy of the output bound for different combinations of N^{pr} and N^{du}. To obtain a maximum relative output bound of approximately 1% for $M = 36$, we require either $(N^{\mathrm{pr}}, N^{\mathrm{du}}) = (10, 50)$, $(30, 30)$, or $(50, 20)$. We may thus select the values of N^{pr} and N^{du} so as to minimize the computational cost involved to obtain a desired accuracy; here, an equal weight on N^{pr} and N^{du} is close to optimal.

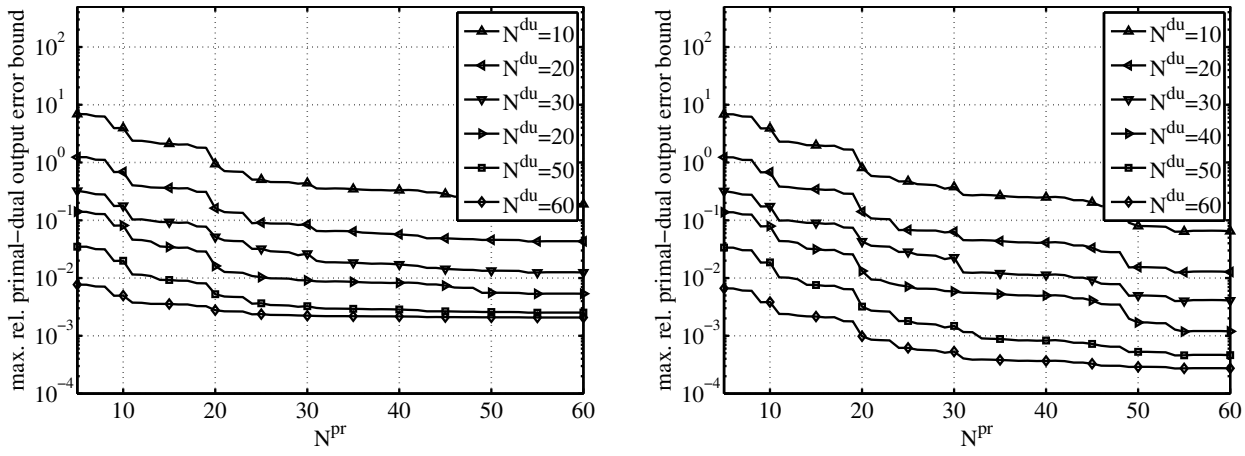

(a) $M = 20$ (b) $M = 36$

Figure 5: Numerical results for the reduced basis method: maximum relative primal-dual output error bound $\Delta^{s,\max,\mathrm{rel}}_{M,N,\mathcal{P}}$ as a function of N^{pr} and N^{du} for $p = 5$, $\Phi = \Phi_2$, and (a) $M = 20$ and (b) $M = 36$.

Finally, we present in Table 4 for a specific combination of N^{pr}, N^{du}, and M the maximum relative truth output errors $\varepsilon^{s,\max,\mathrm{rel}}_{M,N}$, the maximum relative output bound $\Delta^{s,\max,\mathrm{rel}}_{M,N,\mathcal{P}}$, and the average ef-

fectivity $\eta^{s,\text{ave}}_{M,N,\mathcal{P}}$; here, $\varepsilon^{s,\text{max,rel}}_{M,N}$ is the maximum over Ξ_{test} of $\varepsilon^{s,K}_{M,N}(\mu)/|s^K(\mu)|$, $\Delta^{s,\text{max,rel}}_{M,N,\mathcal{P}}$ is the maximum over Ξ_{test} of $\Delta^{s,K}_{M,N,\mathcal{P}}(\mu)/|s^K(\mu)|$, and $\eta^{s,\text{ave}}_{M,N,\mathcal{P}}$ is the average over Ξ_{test} of $\Delta^{s,K}_{M,N,\mathcal{P}}(\mu)/\varepsilon^{s,K}_{M,N}(\mu)$. We also present the online computational times to calculate $s^k_{M,N}(\mu)$ and $\Delta^{s,k}_{N,M,\mathcal{P}}(\mu)$ for $1 \le k \le K$. The values are normalized with respect to the computational time for direct calculation of the truth approximation output $s^k(\mu)$, $1 \le k \le K$. We present the corresponding results for the primal-only approach in Table 5.

We observe that the output approximation and output bound for the primal-dual formulation converge very fast. Furthermore, the primal-dual formulation is clearly superior to the primal-only formulation. To achieve a desired accuracy in the output bound of approximately 1%, we require $N^{\text{pr}} = 30$, $N^{\text{du}} = 30$, and $M = 30$ for the primal-dual formulation. Using the primal-only formulation the output bound is still larger than 10% even if we set N^{pr} and M to their maximum values $N^{\text{pr}}_{\text{max}} = 60$ and $M_{\text{max}} = 50$. The output effectivities are $\mathcal{O}(10^3)$ and thus worse than the effectivities of the energy norm bounds since our bound cannot take into account any correlation between the primal and dual error. Despite the quite large effectivities, however, the computational savings are considerable: the computational time to evaluate the reduced basis output approximation *and* output bound is a factor of $\mathcal{O}(10^4)$ faster than direct calculation of the truth approximation output.

N^{pr}	N^{du}	M	$\varepsilon^{s,\text{max,rel}}_{M,N}$	$\Delta^{s,\text{max,rel}}_{M,N,\mathcal{P}}$	$\eta^{s,\text{ave}}_{M,N,\mathcal{P}}$	comp. time $\forall k$
10	10	10	1.85E-02	4.34E+00	1715	8.46E-05
20	20	20	6.25E-04	1.62E-01	1605	1.08E-04
30	30	30	8.45E-05	2.38E-02	2547	1.39E-04
40	40	30	4.45E-05	5.97E-03	2093	2.02E-04
50	50	36	2.01E-06	5.78E-04	1647	2.58E-04
60	60	36	2.07E-06	2.74E-04	1627	3.29E-04

Table 4: Primal-dual reduced basis output approximation: maximum relative truth output error $\varepsilon^{s,\text{max,rel}}_{M,N}$, maximum relative output error bound $\Delta^{s,\text{max,rel}}_{M,N,\mathcal{P}}$, average effectivity $\eta^{s,\text{ave}}_{M,N,\mathcal{P}}$ and computation times for $p = 5$ and $\Phi = \Phi_2$ as a function of N^{pr}, N^{du} and M. The computation time is normalized with respect to the computation time of calculating the truth output.

N^{pr}	M	$\tilde{\varepsilon}^{s,\mathrm{max,rel}}_{M,N^{\mathrm{pr}}}$	$\tilde{\Delta}^{s,\mathrm{max,rel}}_{M,N^{\mathrm{pr}},\mathcal{P}}$	$\tilde{\eta}^{s,\mathrm{ave}}_{M,N^{\mathrm{pr}},\mathcal{P}}$	comp. time $\forall k$
10	10	2.49E-01	1.79E+01	103	2.72E-05
20	20	9.59E-02	3.30E+00	146	3.87E-05
40	30	6.13E-03	9.97E-01	1959	8.54E-05
60	36	2.96E-03	2.76E-01	1073	1.49E-04

Table 5: Primal-only reduced basis output approximation: maximum relative truth output error $\tilde{\varepsilon}^{s,\mathrm{max,rel}}_{M,N^{\mathrm{pr}}}$, maximum relative output error bound $\tilde{\Delta}^{s,\mathrm{max,rel}}_{M,N^{\mathrm{pr}},\mathcal{P}}$, average effectivity $\tilde{\eta}^{s,\mathrm{ave}}_{M,N^{\mathrm{pr}},\mathcal{P}}$ and computation time for $p = 5$ and $\Phi = \Phi_2$ as a function of M and N^{pr}. The computation time is normalized with respect to the computation time of calculating the truth output.

7. Conclusions

We have presented rigorous *a posteriori* error bounds for reduced basis approximations of problems with non-affine source terms. To this end, we employed the recently proposed rigorous *a posteriori* error bounds for the empirical interpolation method and we developed primal-dual procedures to ensure rapid convergence of the reduced basis output approximation and associated error bound. The error bounds take both error contributions — the error introduced by the reduced basis approximation *and* the error induced by the function interpolation — explicitly into account.

We presented numerical results for a three-dimensional welding process that showed the very fast convergence of the reduced basis approximation and associated error bounds. The computational savings in the online stage are considerable; we observed a speed-up of $\mathcal{O}(10^4)$ in the calculation of the output estimate and bound compared to direct calculation of the truth output.

The primal-dual formulation proved to be clearly superior to the primal-only formulation — the improved convergence rate of the output error and bound led to considerable computational savings for a given desired output accuracy. Similar results have been presented previously for reduced basis approximations of linear affine and quadratically nonlinear problems in [14, 27, 37, 26]. However, in this paper we showed that — in the non-affine case — a small interpolation error and thus large enough dimension of the EIM approximation space is essential in recovering the superconvergence in the output approximation and bound.

A topic of future research is the application of the methods developed here in the solution of the inverse and subsequent online control problem using real experimental data.

Appendix A. Proof of Proposition 2

For simplicity we shall omit the parameter-dependence of the state variables in our notation, i.e. we write y^k instead of $y^k(\mu)$ etc.

First we note that the dual of the output at time t^L, $L = 1, \ldots, K$, satisfies

$$-m(v, \psi_L^{k'+1} - \psi_L^{k'}) + \Delta t\, a(v, \psi_L^{k'+(1-\theta)}; \mu) = 0 \tag{A.1}$$

for all $v \in X$ and $k' = 1, \ldots, L$, with final condition

$$m(v, \psi_L^{L+1}) = l(v) \tag{A.2}$$

for all $v \in X$. We now choose $v = e_{M,N^{\rm pr}}^{y,k'-1+\theta}$ in (A.1) and sum from $k' = 1$ to L to obtain

$$-\sum_{k'=1}^{L} m(e_{M,N^{\rm pr}}^{y,k'-1+\theta}, \psi_L^{k'+1} - \psi_L^{k'}) + \Delta t \sum_{k'=1}^{L} a(e_{M,N^{\rm pr}}^{y,k'-1+\theta}, \psi_L^{k'+(1-\theta)}; \mu) = 0, \tag{A.3}$$

which can be rewritten in the form

$$\sum_{k'=1}^{L} m(e_{M,N^{\rm pr}}^{y,k'} - e_{M,N^{\rm pr}}^{y,k'-1}, \psi_L^{k'+(1-\theta)}) + \Delta t \sum_{k'=1}^{L} a(e_{M,N^{\rm pr}}^{y,k'-1+\theta}, \psi_L^{k'+(1-\theta)}; \mu) = m(e_{M,N^{\rm pr}}^{y,L}, \psi_L^{L+1}), \tag{A.4}$$

where we used the fact that $e_{M,N^{\rm pr}}^{y,0} \equiv 0$. We now note from the final condition of the dual problem (A.2) that $m(e_{M,N^{\rm pr}}^{y,L}, \psi_L^{L+1}) = l(e_{M,N^{\rm pr}}^{y,L})$ to obtain

$$l(e_{N^{\rm pr}}^{y,L}) = \sum_{k'=1}^{L} m(e_{M,N^{\rm pr}}^{y,k'} - e_{M,N^{\rm pr}}^{y,k'-1}, \psi_L^{k'+(1-\theta)}) + \Delta t \sum_{k'=1}^{L} a(e_{M,N^{\rm pr}}^{y,k'-1+\theta}, \psi_L^{k'+(1-\theta)}; \mu). \tag{A.5}$$

We next derive from (18) and (33) that the primal error satisfies

$$\begin{aligned} m(e_{M,N^{\rm pr}}^{y,k'} - e_{M,N^{\rm pr}}^{y,k'-1}, v) + \Delta t\, a(e_{M,N^{\rm pr}}^{y,k'-1+\theta}, v; \mu) & \\ = \Delta t\, r_{N^{\rm pr}}^{y,k'}(v; \mu) + \Delta t\, f(v; g(\mu) - g_M(\mu)) u^{k'-1+\theta} & \end{aligned} \tag{A.6}$$

for all $v \in X$ and $k' = 1, \ldots, K$. Choosing $v = \psi_L^{k'+(1-\theta)}$ and summing from $k' = 1$ to L it follows that

$$\begin{aligned} \sum_{k'=1}^{L} m(e_{M,N^{\rm pr}}^{y,k'} - e_{M,N^{\rm pr}}^{y,k'-1}, \psi_L^{k'+(1-\theta)}) + \Delta t \sum_{k'=1}^{L} a(e_{M,N^{\rm pr}}^{y,k'-1+\theta}, \psi_L^{k'+(1-\theta)}; \mu) & \\ = \Delta t \sum_{k'=1}^{L} r_{N^{\rm pr}}^{y,k'}(\psi_L^{k'+(1-\theta)}; \mu) + \Delta t \sum_{k'=1}^{L} f(\psi_L^{k'+(1-\theta)}; g(\mu) - g_M(\mu)) u^{k'-1+\theta}. & \end{aligned} \tag{A.7}$$

From (A.5) and (A.7) we have

$$l(e^{y,L}_{N^{\rm pr}}) = \Delta t \sum_{k'=1}^{L} r^{y,k'}_{N^{\rm pr}}(\Psi^{K-L+k'+(1-\theta)};\mu) + \Delta t \sum_{k'=1}^{L} f(\Psi^{K-L+k'+(1-\theta)}; g(\mu)-g_M(\mu))u^{k'-1+\theta}, \quad \text{(A.8)}$$

where we used the shifting property of the dual (23). From the definition of the truth output, $s^k(\mu)$, the reduced basis output approximation, $s^k_{M,N}(\mu)$, and (A.8) we now obtain

$$s^k(\mu) - s^k_{M,N}(\mu) = \Delta t \sum_{k'=1}^{k} r^{y,k'}_{N^{\rm pr}}(e^{\Psi,K-k+k'+(1-\theta)}_{N^{\rm du}}(\mu);\mu) + \Delta t \sum_{k'=1}^{k} f(\Psi^{K-k+k'+(1-\theta)}(\mu); g(\mu)-g_M(\mu))u^{k'-1+\theta}. \quad \text{(A.9)}$$

Using the definition of the dual norm the first term of the right hand side of (A.9) is bounded by

$$\left|\Delta t \sum_{k'=1}^{k} r^{y,k'}_{N^{\rm pr}}(e^{\Psi,K-k+k'+(1-\theta)}_{N^{\rm du}}(\mu);\mu)\right| \leq \Delta t \sum_{k'=1}^{k} \left\| r^{y,k'}_{N^{\rm pr}}(\cdot;\mu)\right\|_{X^*} \left\| e^{\Psi,K-k+k'+(1-\theta)}_{N^{\rm du}}(\mu)\right\|_X, \quad \text{(A.10)}$$

and using the Cauchy-Schwarz inequality it follows that

$$\left|\Delta t \sum_{k'=1}^{k} r^{y,k'}_{N^{\rm pr}}(e^{\Psi,K-k+k'+(1-\theta)}_{N^{\rm du}}(\mu);\mu)\right| \leq \left(\frac{\Delta t}{\alpha^{\rm LB}_a(\mu)} \sum_{k'=1}^{k} \left\| r^{y,k'}_{N^{\rm pr}}(\cdot;\mu)\right\|^2_{X^*}\right)^{\frac{1}{2}} \times \left(\Delta t\, \alpha^{\rm LB}_a(\mu) \sum_{k'=1}^{k} \left\| e^{\Psi,K-k+k'+(1-\theta)}_{N^{\rm du}}(\mu)\right\|^2_X\right)^{\frac{1}{2}}. \quad \text{(A.11)}$$

By definition, the first term of the right hand side of (A.11) is equal to the error bound $\Delta^{y_M,k}_{N^{\rm pr}}(\mu)$ of the affine primal problem (21), and the second term satisfies

$$\Delta t\, \alpha^{\rm LB}_a(\mu) \sum_{k'=1}^{k} \left\| e^{\Psi,K-k+k'+(1-\theta)}_{N^{\rm du}}(\mu)\right\|^2_X \leq \left(\Delta^{\Psi,K-k+1}_{N^{\rm du}}(\mu)\right)^2. \quad \text{(A.12)}$$

We now turn to the second term of the right hand side of (A.9), which we can bound by

$$\begin{aligned}\Delta t \sum_{k'=1}^{k} & f(\Psi^{K-k+k'+(1-\theta)}(\mu); g(\mu) - g_M(\mu)) u^{k'-1+\theta} \\ & \leq \Delta t \sum_{k'=1}^{k} \left\| e_{N^{\mathrm{du}}}^{\Psi, K-k+k'+(1-\theta)}(\mu) \right\|_X \sup_{v \in X} \frac{f(v; g(\mu) - g_M(\mu))}{\|v\|_X} \left| u^{k'-1+\theta} \right| \\ & \qquad + \Delta t \sum_{k'=1}^{k} f(\Psi_{N^{\mathrm{du}}}^{K-k+k'+(1-\theta)}(\mu); g(\mu) - g_M(\mu)) u^{k'-1+\theta}. \quad \text{(A.13)}\end{aligned}$$

With the help of the rigorous EIM-bound $\delta_{M,p,\Phi}^{g}$ this can be simplified to

$$\begin{aligned}\Delta t \sum_{k'=1}^{k} & f(\Psi^{K-k+k'+(1-\theta)}(\mu); g(\mu) - g_M(\mu)) u^{k'-1+\theta} \\ & \leq \Delta t \, \delta_{M,p,\Phi}^{g} \left\| f(\cdot; 1) \right\|_{X^*} \sum_{k'=1}^{k} \left\| e_{N^{\mathrm{du}}}^{\Psi, K-k+k'+(1-\theta)}(\mu) \right\|_X \left| u^{k'-1+\theta} \right| \\ & \qquad + \Delta t \, \delta_{M,p,\Phi}^{g} \sum_{k'=1}^{k} \left| f(\Psi_{N^{\mathrm{du}}}^{K-k+k'+(1-\theta)}(\mu); 1) u^{k'-1+\theta} \right|. \quad \text{(A.14)}\end{aligned}$$

Finally, using the Cauchy-Schwarz inequality, the coercivity of a and the definition of the dual spatio-temporal energy norm and the dual error bound, we have

$$\Delta t \sum_{k'=1}^{k} \left\| e_{N^{\mathrm{du}}}^{\Psi, K-k+k'+(1-\theta)}(\mu) \right\|_X \left| u^{k'-1+\theta} \right| \leq \Delta_{N^{\mathrm{du}}}^{\Psi, K-k+1}(\mu) \left(\frac{\Delta t}{\alpha_a^{\mathrm{LB}}(\mu)} \sum_{k'=1}^{k} \left(u^{k'-1+\theta} \right)^2 \right)^{\frac{1}{2}}. \quad \text{(A.15)}$$

The result directly follows from (A.9)-(A.15). □

Acknowledgements

This work was supported by the Excellence Initiative of the German federal and state governments and the German Federation of Industrial Research Associations funded by the German Federal Ministry of Economics and Technology.

References

[1] T. W. Eagar, N. S. Tsai, Temperature fields produced by traveling distributed heat sources, Welding Journal 62 (1983) S346–S355.

[2] J. Goldak, M. Bibby, J. Moore, R. House, B. Patel, Computer modeling of heat flows in welds, Metall. Mater. Trans. B 17B (1985) 587–600.

[3] J.-B. Song, D. E. Hardt, Dynamic modeling and adaptive control of the gas metal arc welding process, J. Dyn. Syst. Meas. Control 116 (1994) 405–413.

[4] S. Wang, J. Goldak, J. Zhou, S. Tchernov, D. Downey, Simulation on the thermal cycle of a welding process space-time convection-diffusion finite element analysis, Int. J. Therm. Sci. 48 (2009) 936–947.

[5] K. Kazemi, J. Goldak, Numerical simulation of laser full penetration welding, Comput. Mat. Sci. 44 (2009) 841–849.

[6] J. Goldak, A. Chakravarti, M. Bibby, A new finite element model for welding heat sources, Metall. Mater. Trans. B 15B (1984) 299–305.

[7] V. A. Karkhin, P. N. Homich, V. G. Michailov, Models for volume heat sources and functional-analytical technique for calculating the temperature fields in butt welding, in: Mathematical Modelling of Weld Phenomena 8, Verlag der Technischen Universität Graz, 2007, pp. 819–834.

[8] V. Akçelik, G. Biros, A. Drăgănescu, O. Ghattas, J. Hill, B. van Bloemen Waanders, Dynamic data driven inversion for terascale simulations: Real-time identification of airborne contaminants, in: Proc. of the 2005 ACM/IEEE Conference on Supercomputing.

[9] O. Bashir, K. Willcox, O. Ghattas, B. van Bloemen Waanders, J. Hill, Hessian-based model reduction for large-scale systems with initial-condition inputs, Int. J. Numer. Meth. Engng. 73 (2008) 844–868.

[10] L. Dede, A. Quarteroni, Optimal control and numerical adaptivity for advection-diffusion equations, ESAIM, Math. Model. Numer. Anal. 39 (2005) 1019–1040.

[11] V. A. Karkhin, V. V. Plochikhine, H. W. Bergmann, Solution of inverse heat conduction problem for determining heat input, weld shape, and grain structure during laser welding, Sci. Technol. Weld. Joi. 7 (2002) 224–231.

[12] J.-B. Song, D. E. Hardt, Closed-loop control of weld pool depth using a thermally based depth estimator, Welding Journal 72 (1993) S471–S478.

[13] J.-B. Song, D. E. Hardt, Estimation of weld bead depth for in-process control, in: Automation of Manufacturing Processes, volume DSC-22 of *ASME Winter Annual Meeting*, pp. 39–45.

[14] G. Rozza, D. Huynh, A. Patera, Reduced basis approximation and a posteriori error estimation of affinely parametrized elliptic coercive partial differential equations, Arch. Comput. Meth. Eng. 15 (2008) 229–275.

[15] M. Barrault, Y. Maday, N. C. Nguyen, A. T. Patera, An empirical interpolation method: Application to efficient reduced-basis discretization of partial differential equations, C. R. Acad. Sci. Paris Sér. I 339 (2004) 667–672.

[16] M. A. Grepl, Y. Maday, N. C. Nguyen, A. T. Patera, Effcient reduced-basis treatment of nonaffine and nonlinear partial differential equations, ESAIM, Math. Model. Numer. Anal. 41 (2007) 575–605.

[17] N. C. Nguyen, A posteriori error estimation and basis adaptivity for reduced-basis approximation of nonaffine-parametrized linear elliptic partial differential equations, J. Comput. Phys. 227 (2007) 983–1006.

[18] T. M. Lassila, G. Rozza, Parametric free-form shape design with pde models and reduced basis method, Comput. Meth. Appl. Mech. Eng. 199 (2010) 1583–1592.

[19] C. Canuto, T. Tonn, K. Urban, A-posteriori error analysis of the reduced basis method for non-affine parameterized nonlinear pde's, SIAM J. Numer. Anal. 47 (2009) 2001–2022.

[20] M. A. Grepl, Certified reduced basis methods for nonaffine linear time-varying and nonlinear parabolic partial differential equations, 2011. Accepted for publication.

[21] J. L. Eftang, M. A. Grepl, A. T. Patera, A posteriori error bounds for the empirical interpolation method, C. R. Acad. Sci. Paris Sér. I 348 (2010) 575–579.

[22] N. Pierce, M. Giles, Adjoint recovery of superconvergent functionals from pde approximations, SIAM Review 42 (2000) 247–264.

[23] R. Becker, R. Rannacher, Weighted a posteriori error control in finite element methods, in: ENUMATH 95 Proc, World Sci. Publ. Singapore, 1997.

[24] A. Patera, E. Rønquist, A general output bound result: application to discretization and iteration error estimation and control, Math. Model. Meth. Appl. Sci. 11 (2001) 685–712.

[25] C. Prud'homme, D. Rovas, K. Veroy, Y. Maday, A. T. Patera, G. Turinici, Reliable real-time solution of parametrized partial differential equations: Reduced-basis output bound methods, J. Fluids Eng. (2002) 70–80.

[26] D. V. Rovas, L. Machiels, Y. Maday, Reduced-basis output bound methods for parabolic problems, IMA J. Num. Anal. 26 (2006) 423–445.

[27] M. Grepl, A. Patera, A posteriori error bounds for reduced-basis approximations of parametrized parabolic partial differential equations, ESAIM, Math. Model. Numer. Anal. 39 (2005) 157–181.

[28] Y. Maday, N. C. Nguyen, A. T. Patera, G. S. H. Pau, A general multipurpose interpolation procedure: The magic points, Comm. Pure Appl. Anal. 8 (2009) 383–404.

[29] A. Quarteroni, R. Sacco, F. Saleri, Numerical Mathematics, volume 37 of *Texts in Applied Mathematics*, Springer, New York, 1991.

[30] J. Eftang, M. Grepl, A. Patera, E. Rønquist, Approximation of parametric derivatives by the empirical interpolation method, In preparation (2011).

[31] A. Quarteroni, A. Valli, Numerical Approximation of Partial Differential Equations, Springer, 2nd edition, 1997.

[32] D. B. P. Huynh, G. Rozza, S. Sen, A. Patera, A successive constraint linear optimization method for lower bounds of parametric coercivity and inf-sup stability constants, C. R. Acad. Sci. Paris Sér. I 345 (2007) 473–478.

[33] K. Veroy, D. Rovas, A. T. Patera, A posteriori error estimation for reduced-basis approximation of parametrized elliptic coercive partial differential equations: "Convex inverse" bound conditioners, ESAIM, Control Optim. Calc. Var. 8 (2002) 1007–1028. Special Volume: A tribute to J.-L. Lions.

[34] B. Haasdonk, M. Ohlberger, Reduced basis method for finite volume approximations of parametrized linear evolution equations, ESAIM, Math. Model. Numer. Anal. 42 (2008) 277–302.

[35] D. Knezevic, A. Patera, A certified reduced basis method for the Fokker-Planck equation of dilute polymeric fluids: FENE dumbbells in extensional flow, SIAM J. Sci. Comput. 32 (2010) 793–817.

[36] L. Sirovich, Turbulence and the dynamics of coherent structures, part 1: Coherent structures, Q. Appl. Math. 45 (1987) 561–571.

[37] K. Veroy, A. T. Patera, Certified real-time solution of the parametrized steady incompressible Navier-Stokes equations: rigorous reduced-basis a posteriori error bounds, Int. J. Num. Meth. Fluids 47 (2005) 773–788.